Molecular Dynamics Study of *p-tert*-Butylcalix[4]arenetetraamide and Its Complexes with Neutral and Cationic Guests. Influence of Solvation on Structures and Stabilities

P. Guilbaud, A. Varnek, and G. Wipff*

Contribution from the URA 422 CNRS, Institut de Chimie, 4, rue Blaise Pascal, 67000 Strasbourg, France

Received March 5, 1993

Abstract: A series of molecular dynamics simulations have been performed on *tert*-butylcalix[4]arenetetraamide ligand L, with neutral or anionic guests inside the cone (MeOH, MeCN, H_2O, SCN^-) or with cations (Li^+–Cs^+, Eu^{3+}) in the pseudocavity at the lower rim. The uncomplexed ligand L is found to be not preorganized *in vacuo* or in water to complex cations at the lower rim. The structure and dynamics of LM^{n+} complexes differ from the solid-state picture of the LK^+ complex. They depend on the size and charge of the cation and on solvation effects. In aqueous solution, the M^{n+}/ligand attractions compete with the hydration of the partially encapsulated ion and the carbonyl binding sites, leading to an equilibrium of conformers with more or less converging binding sites. A detailed analysis of the hydration pattern and dynamics features of the apolar cone and of the hydrophilic moiety is presented. A guest-dependent dynamic coupling between the motions of the cone and of the lower-rim oxygens is demonstrated. In the LEu^{3+} complex, one water molecule is co-complexed with Eu^{3+}. In the gas phase, a binding selectivity is predicted for Li^+ over other alkali cations. In water, no firm conclusion can be drawn due to the flexibility of the lower-rim binding sites and related sampling problems.

Introduction

Calixarenes[1,2] are macrocyclic host molecules built from phenolic units which can bind a variety of guests. They can be easily synthesized and modified with good yields, leading to derivatives with selected properties. Unsubstituted calixarenes are not effective cation receptors, whereas their derivatives with amides, ketones, and esters as substituents at the lower rim (Chart I) have significant cation affinities.[3-9] Carbonyl-containing calix[4]arenes (Chart I) selectively bind Na^+ in methanol[10,11] and extract Na^+ at water/CH_2Cl_2[10,12-17] or water/$CHCl_3$ interfaces.[3] In acetonitrile, ketone, and ester, calix[4]arenes[11,13] selectively bind Li^+ over other alkali cations. The amide derivative L (R = NEt_2, Chart I) forms stable complexes with Eu^{3+}, Tb^{3+}, and Gd^{3+} chlorides[18,19] in water or in alcohols.

Chart I. Carbonyl-Containing Calix[4]arenes

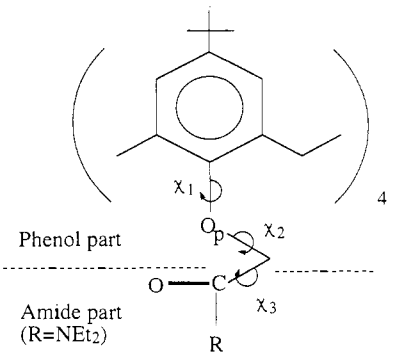

These calix[4]arenes adopt a cone conformation (defined by the +−, +−, +−, +− symbolic representation[20]) with two separated binding regions. First, the apolar cone can accommodate neutral guests. Related examples in the solid state involve benzene, xylene, anisole,[21] toluene,[22] chloroform,[23] acetonitrile,[24] and some others[25] when calix[4]arenes are uncomplexed at the

(1) *Calixarenes: a versatile class of macrocyclic compounds*; Vicens, J., Böhmer, V., Eds.; Kluwer Academic Publishers: Dordrecht, The Netherlands, 1991.
(2) Gutsche, C. D. *Calixarenes*; The Royal Society of Chemistry: Cambridge, 1989.
(3) Arduini, A.; Ghidini, E.; Ponchini, A.; Ungaro, R.; Andreetti, G. D.; Calestani, G.; Ugozzoli, F. *J. Inclusion Phenom.* **1988**, *6*, 119–134.
(4) Arduini, A.; Casnati, A.; Fabbi, M.; Minari, P.; Pochini, A.; Sicuri, A. R.; Ungaro, R. In *Supramolecular chemistry*; Balzani, V., Cola, L. D., Eds.; Kluwer Academic Publishers: Dordrecht, The Netherlands, 1992; pp 31–50.
(5) Arnaud-Neu, F.; Schwing-Weil, M. J.; Ziat, K.; Cremin, S.; Harris, S. J.; Kervey, M. A. M. *New J. Chem.* **1991**, *15*, 33–37.
(6) Arnaud-Neu, F.; Cremin, S.; Cunningham, D.; Harris, S. J.; McArdle, P.; McKervey, A.; McManus, M.; Schwing-Weill, M.-J.; Ziat, K. *J. Inclusion Phenom. Mol. Recogn.* **1991**, *10*, 329–339.
(7) Ungaro, R.; Pochini, A. *Frontiers In Supramolecular Organic Chemistry and Photochemistry*; VCH: Weinheim, 1991; pp 57–80.
(8) Ungaro, R.; Ponchini, A.; Arduini, A. In *Inclusion Phenomena and Molecular Recognition*; Atwood, J., Ed.; Plenum Press: New York, 1990.
(9) Ungaro, R.; Pochini, A. In *Calixarenes: a versatile class of macrocyclic compounds*; Vicens, J., Bohmer, V., Eds.; Kluwer Academic Publishers: Dordrecht, The Netherlands, 1991; pp 127–147.
(10) Arnaud-Neu, F.; Collins, E. M.; Deasy, M.; Ferguson, G.; Harris, S. J.; Kaitner, B.; Lough, A. J.; McKervey, M. A.; Marques, E.; Ruhl, B. L.; Schwing-Weil, M. J.; Seward, E. M. *J. Am. Chem. Soc.* **1989**, *111*, 8681–8691.
(11) de Namor, A. F. D.; Sueros, N. A. D.; McKervey, M. A.; Barrett, G.; Arnaud-Neu, F. A.; Schwing-Weill, M. J. *J. Chem. Soc., Chem. Commun.* **1991**, 1546–1548.
(12) McKervey, M. A.; Seward, E. M.; Ferguson, G.; Ruhl, B.; Harris, S. J. *J. Chem. Soc., Chem. Commun.* **1985**, 388.
(13) Schwing-Weill, M. J.; Arnaud-Neu, F.; McKervey, M. A. *J. Phys. Org. Chem.* **1992**, *5*, 496–501.
(14) Chang, S.-K.; Cho, I. *Chem. Lett.* **1984**, 477.
(15) Chang, S.-K.; Cho, I. *J. Chem. Soc., Perkin Trans. 1* **1986**, 211.
(16) Ferguson, G.; Kaitner, B.; McKervey, M. A.; Seward, E. M. *J. Chem. Soc., Chem. Commun.* **1987**, 584.
(17) Calestani, G.; Ugozzoli, F.; Arduini, A.; Ghidini, E.; Ungaro, R. *J. Chem. Soc., Chem. Commun.* **1987**, 344.
(18) Sabbatini, N.; Guardigli, M.; Mecati, A.; Balzani, V.; Ungaro, R.; Ghidini, E.; Casnati, A.; Pochini, A. *J. Chem. Soc.* **1990**, 878.
(19) Sabbatini, N.; Mecati, A.; Guardigli, M.; Balzani, V.; Lehn, J. M.; Zeissel, R.; Ungaro, R. *J. Lumin.* **1991**, *48,49*, 463–468.
(20) Ugozzoli, F.; Andreetti, G. D. *J. Inclusion Phenom. Mol. Recogn.* **1992**, *13*, 337–348.
(21) Coruzzi, M.; Andreeti, G. D.; Bocchi, V.; Pochini, A.; Ungaro, R. *J. Chem. Soc., Perkin Trans. 2* **1982**, 1133.

0002-7863/93/1515-8298$04.00/0

lower rim and toluene or methanol[3,26] with their cation complexes. Second, at the lower rim, the hydrophilic moiety is flexible enough to define a pseudocavity to complex cations for converging (C) orientations of carbonyl binding sites. It can also interact effectively with solvent molecules for diverging (D) orientations of the carbonyls.

In solution the precise conformation of carbonyl-containing calixarenes and their complexes is not well defined, concerning particularly the shapes of the cone and the hydrophilic pseudocavity. We do not know to what extent it is guest- and solvent-dependent. To what extent is the solid-state picture of the LK^+ complex representative of other complexes? Can the solvent interact with the complexed cation, as in the case of cryptates?[27] Can solvation compete with the cation in determining the conformation of its binding sites? Can the solvent fill the cone and "preorganize" the host for complexation?[11]

Our aim is to investigate these questions by molecular dynamics (MD) simulations on calixarenes with one guest inside the cone and/or with cations complexed at the lower rim, first in the gas phase and then in aqueous solution. From a thermodynamic point of view, it is also important to rationalize the relative binding selectivities, as a result of "intrinsic binding affinities" (from the cation–calixarene interactions *in vacuo*) and/or solvation effects. The extraction selectivity is another important issue which results from the complex interplay between stabilities and solubilities of the complexes in two liquid phases.

To our knowledge this is the first theoretical study on calixarenes with substituents at the lower rim carrying cation binding sites like carbonyls. In particular, the questions of mutual influence of the guests in hydrophilic and hydrophobic parts of the ligand and of the influence of solvents on the conformational state of calixarenes and their complexes have not been addressed so far. Previous computational work involved the molecular mechanics (MM) and MD calculations of Grootenhuis *et al.*[28] on calix[4]-arenes and their tetramethyl ethers with alkyl substituents at the upper rim. Royer *et al.*[29] performed on a MM study of the interconversion of the cone of the unsubstituted calix[4]arene. Andreetti *et al.* studied by MM the interaction of pyridine with a calix–crown.[30] Kollman and Miyamoto used MD and free energy perturbation simulations to study the complexation selectivity of conformationally rigid calixspherands.[31]

More specifically, we consider the *p-tert*-butylcalix[4]-arenetetraamide (L) uncomplexed, and complexed with the Li^+, Na^+, K^+, Cs^+, and Eu^{3+} cations at the lower rim, and/or complexed with neutral (H_2O, MeOH, MeCN) and anionic (SCN^-) guests inside the cone. This ligand L has been chosen because of the availability of thermodynamic data on its complexation and extraction capabilities.[13] There are also X-ray data for the free molecule L and for its KSCN or KI complexes in the solid state.[3] Compared to ester and ketone analogs, the tetraamide forms alkali cation complexes of higher stability.[13] It is also representative of ionophores able to transduce directly the complexation of heavy-metal ions into an electric signal (CHEMFETs[79]).

Although LM^+ complexes are not soluble in pure water, we performed calculations in water for the following reasons. First, we want to compare the hydration of the "hydrophobic" and "hydrophilic" units and assess their relative contributions to the total hydration energy, in relation with the solubility problem. Second, during extraction experiments, the organic phase containing L and LM^+ is saturated with water, whose concentration (about 0.05 M on the average[32]) is large compared to that of the ligand (2.5×10^{-4} M[13]). Locally, this concentration can still be larger,[33] leading to a possible microscopic solvation of the ionophore. Even in chloroform, water can effectively solvate ligands and influence the thermodynamics of host–guest complexation.[34] Water also has obvious similarities with methanol, in which experiments have been carried out, especially as far as the coordination of cations is concerned.[35] Another issue is the effect of remote solubilizing groups on the binding affinities and selectivities. For instance, replacement of *tert*-butyl groups of L by SO_3^- groups (to our knowledge not achieved so far experimentally) would make the complex water soluble. We are actually simulating these SO_3^- analogs in water to address this important question. The results reported here serve also as a reference for the behavior in nonaqueous solutions, currently under investigation.[36]

Computational Procedures

Molecular dynamics calculations were performed with the program AMBER4[37] using the representation of the potential energy from ref 38. The parameters for intramolecular and nonbonded intermolecular interactions have been taken from refs 27 and 38.

Choice of Charges. The atomic charges Q_i obtained by the least-squares method reproduce the molecular electrostatic potential (ESP) on the Connolly surfaces,[39] computed by the MNDO method.[40] The charges for L have been calculated on the fragment displayed in Chart II, with further averaging of Q_i. They were multiplied by 1.42, which scales MNDO ESP charges to the *ab initio* (6-31G*) values.[41] The carbonyl and phenolic oxygens were fixed in a *trans* conformation to avoid overlap of their contributions.[42] The $Q_{O\text{-phenolic}}$ charges are similar to those obtained by the *ab initio* calculations of Grootenhuis *et al.*[28] with a 6-31G* basis set. $Q_{O\text{-carbonyl}}$ (–0.61) is close to the value (–0.55) derived from free energy perturbation[43] calculations on valinomycin complexes.[44]

The charges of MeOH and MeCN (Chart II) are close to the OPLS values reported in refs 45 and 46. For water we used TIP3P charges[47] which were almost the same as the ESP charges. The 1,4 electrostatic and van der Waals interactions have been calculated without a scaling factor. The residue-based cutoff for nonbonded interactions was set at 8 Å using periodic boundary conditions.

(22) Andreeti, G. D.; Ungaro, R.; Pochini, A. *J. Chem. Soc., Chem. Commun.* **1979**, 1005–1007.
(23) Gutsche, C. D.; Dhavan, B.; No, K. H.; Muthukrishman, R. *J. Am. Chem. Soc.* **1981**, *103*, 3782–3792.
(24) McKervey, M. A.; Seward, E. M.; Ferguson, G.; Ruhl, B. L. *J. Org. Chem.* **1986**, *51*, 3581–3584.
(25) Atwood, J. L. *Second Summer School on Supramolecular Chemistry, Lecture Notes*; Bishenberg, France, 1992.
(26) Bott, S. G.; Coleman, A. W.; Atwood, J. L. *J. Am. Chem. Soc.* **1986**, *108*, 1709–1710.
(27) Auffinger, P.; Wipff, G. *J. Am. Chem. Soc.* **1991**, *113*, 5976–5988.
(28) Grootenhuis, P. D. J.; Kollman, P. A.; Groenen, L. C.; Reinhoudt, D. N.; Hummel, G. J. V.; Ugozolli, F.; Andreetti, G. D. *J. Am. Chem. Soc.* **1990**, *112*, 4165–4176.
(29) Royer, J.; Bayard, F.; Decoret, C. *J. Chim. Phys.* **1990**, *87*, 1695–1700.
(30) Andreetti, G. D.; Ori, O.; Ugozzoli, F.; Alfieri, C.; Pochini, A.; Ungaro, R. *J. Inclusion Phenom.* **1988**, *6*, 523–536.
(31) Miyamoto, S.; Kollman, P. A. *J. Am. Chem. Soc.* **1992**, *114*, 3668–3674.
(32) *Handbook on Chemistry Russia*; Khimiya Publishing House: Moscow, 1964; Vol. 1, p 662.
(33) Kessler, Y. M.; Zaytsev, A. L. *Solvophobic effects*; Khimiya Publishing House: Moscow, 1989; p 309.
(34) Adrian, J. C.; Wilson, C. S. *J. Am. Chem. Soc.* **1991**, *113*, 678–680.
(35) Chandrasekhar, J.; Jorgensen, W. G. *J. Chem. Phys.* **1982**, *77*, 5080–5089.
(36) Varnek, A. A.; Wipff, G. *J. Phys. Chem.*, in press.
(37) Pearlman, D. A.; Case, D. A.; Cadwell, C. J.; Seibel, G. L.; Singh, U. C.; Weiner, P.; Kollman, P. A. *AMBER4*; University of California, 1991.
(38) Weiner, S. J.; Kollman, P. A.; Nguyen, D. T.; Case, D. A. *J. Comput. Chem.* **1986**, *7*, 230–252.
(39) Connolly, M. A. *J. Appl. Crystallogr.* **1983**, *16*, 548.
(40) *MOPAC-5*; *QCPE Program No. 589*, **1990**.
(41) Besler, B. H.; Merz, K. M.; Kollman, P. A. *J. Comput. Chem.* **1990**, *11*, 431–439.
(42) Woods, R. J.; Khalil, M.; Pell, W.; Moffat, S. H.; Smith, V. H., Jr. *J. Comput. Chem.* **1990**, *11*, 297–310.
(43) van Gunsteren, W. F.; Berendsen, H. J. C. *Comput. Aided Mol. Des.* **1987**, *1*, 171.
(44) Eisenman, G.; Alvarez, O.; Aquist, J. *J. Inclusion Phenom. Mol. Recogn.* **1992**, *12*, 22–53.
(45) Jorgensen, W. L. *J. Phys. Chem.* **1986**, *90*, 1276–1284.
(46) Jorgensen, W. L.; Briggs, J. M. *Mol. Phys.* **1988**, *63*, 547–558.
(47) Jorgensen, W. L.; Chandrasekhar, J.; Madura, J. D. *J. Chem. Phys.* **1983**, *79*, 926–936.

Chart II. Charge Distributions

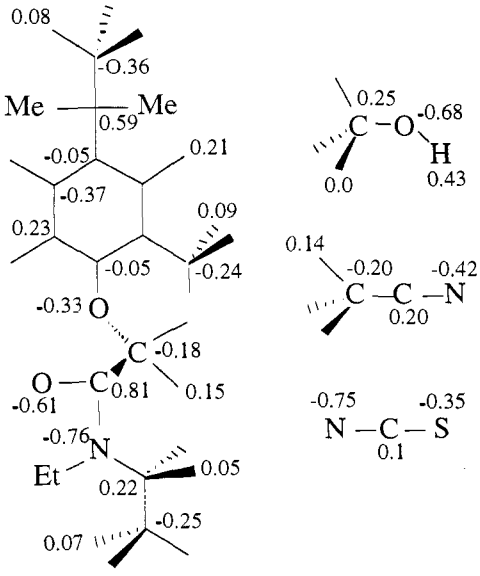

Choice of Geometries. The three forms L(C), L(D), and L-free shown in Figure 1 have been used as starting structures. L-free and L(C) are the X-ray structures of the ligand and of its complex with KSCN, respectively.[3] L(C) has been used for all cation complexes. In L(C), all carbonyl groups are converging more or less toward the cation. Torsional angles are $\chi_2 = 148°$, $\chi_3 = -12°$ (see Chart I), and the cone has a C_{4v} symmetry. The model-built L(D) conformer ($\chi_2 = 80°$, $\chi_3 = -120°$) has a C_{4v} cone and four diverging carbonyl groups. The L-free is of 2-fold symmetry. Its cone has a C_{2v} elongated shape, and amide orientations ($\chi_2 = -95°$, $\chi_3 = -60°$ or 20°) are such that two opposed carbonyls only are clearly diverging. Two of the aromatic rings are nearly parallel to each other, and the two others are nearly perpendicular. Schematically, with respect to the C_2 or C_4 symmetry axis, the amide chains may be either parallel ("axial") or perpendicular ("equatorial"). In L(C) the four chains are axial, in L(D) they are equatorial, and in L-free two are axial and two are equatorial. The L(D) form is expected to be better solvated than L(C) or L-free, and this allows us to test the stability of a regular cone of 4-fold symmetry, compared to an "elongated" C_{2v} cone.

Molecular Dynamics. In the simulations in aqueous solution, the solute has been placed at the center of a water box containing 1000–1100 water molecules (see Tables IV–VIII). After 1000 steps of conjugate gradient minimization, the system was equilibrated for 5 ps of MD at 300 K and 1 atm starting with random velocities. This was followed by 70–300 ps of MD (see Table I). The Verlet algorithm was used with a time step of 2 fs. The SHAKE procedure was applied to constrain all covalent bonds involving a hydrogen atom to their equilibrium length. The temperature was maintained at 300 K by velocity scaling using a relaxation time of 0.1 ps.

Most simulations of the LM^{n+} complexes in water (200–300 ps) starting from the L(C) conformation led to reorientations of the carbonyl side chains. Additional simulations (70–100 ps), starting with the L(D) form, were rerun in order to test the possibility of cation encapsulation along the molecular dynamics and to compare the hydration of these converging/diverging forms.

Free Energy Calculations. We used the windowing technique to obtain the differences of free energies between LM^+ and LM'^+ complexes.[43] The simulation times are reported later in Table X. In the gas phase, the mutations have been performed for 50 ps starting from the L(C) conformers after equilibration. Some were rerun for 200 ps. In water the system was first equilibrated for 50 ps of MD, starting from the L(C) forms. The hydride potential energy from M^+ to M'^+ is $V_\lambda = (1-\lambda)V_{M^+} + \lambda V_{M'^+}$. Each perturbation run consisted of 11 windows. At each window, 500 steps of equilibration and 2000 data collection steps were performed. The total time per perturbation run was 55 ps. In each run, the ΔG was accumulated forward ($\lambda = 1 \rightarrow 0$) and backward ($\lambda = 0 \rightarrow 1$). Additional tests (Table X) involved the L(D) starting form to investigate the influence of the starting structure (after 20 ps of equilibration, 11 windows) or longer perturbation times (105 ps, 21 windows).

One picosecond of simulation took about 1 h of CPU time on a Silicon Graphics 4D-320 station or about 0.5 h on an IBM-3090-600VF. The MD DRAW graphics software was used both for the visualization of the molecular structures and to analyze the structural and energy results.[48]

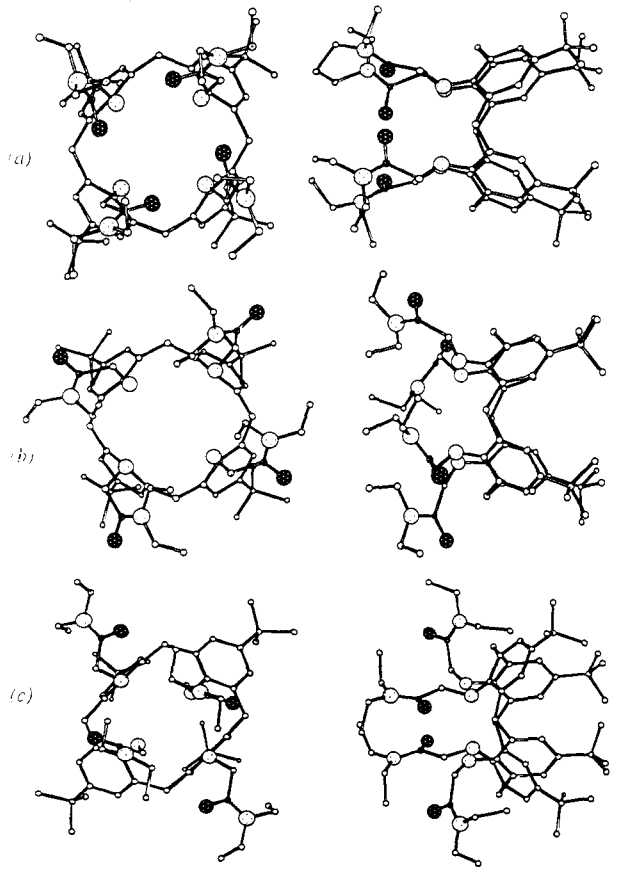

Figure 1. Converging L(C) (a), diverging L(D) (b) and L-free (c) starting structures of calix[4]arenetetraamide (orthogonal view).

Table I. Time (ps) of MD Simulation of Molecule L and Its Complexes in the Gas Phase and in Water

	ligand form			
	gas phase		water	
guest	L(C)	L(D)	L(C)	L(D)
none[a]	50	300 (200)[g]	15 (45)[b]	50
Li^+	50	50	250	70
Na^+	200	50	300	70
K^+	50	50	260 (80)[c]	70
Cs^+	50	50	200	70
Eu^{3+}			120	70
S[d,e]		100		
Na^+, S[d,f]	50	100		
M^+NCS		50		

[a] The L-free form has been simulated 50 ps in the gas phase, 25 ps in water (without constraints), and 15 ps[b] with constraints. [b] All atoms are constrained with force constant of $k = 5$ kcal/(mol/Å^2). [c] For LK^+ with $\chi_2 = 180°$, $\chi_3 = 0°$. [d] S = H_2O, MeOH, MeCN. [e] 300 ps for L = H_2O. [f] 300 ps for L(D) = Na^+, MeCN. [g] Simulation at $T = 800$ K.

Analysis of Results. We characterize the shape of the cone by the distances between opposite central $C_{tert\text{-}butyl}$ carbons. Its symmetry is either C_{2v} or C_{4v}, but taking the amide groups into account may lower the symmetry of L. Although the precise orientation of the amide groups is defined precisely by the torsional angles χ_1–χ_3 (Chart I), we use an i/j index to characterize roughly the number of converging/diverging carbonyl binding sites. For instance, the L(C) form is 4/0, and the L(D) and L-free forms are 0/4 (Figure 1).

The cation's location is defined by its distance $M^{n+}\cdots(O_p)$ from the average plane of phenolic oxygens and by the distances $M^{n+}\cdots O_p$ and $M^{n+}\cdots O_a$ between M^{n+} and the phenolic and amide oxygens, respectively.

(48) Engler, E.; Wipff, G. *MD DRAW. A Program of graphical representation of a molecular trajectories*; Université Louis Pasteur: Strasbourg, France, 1992.

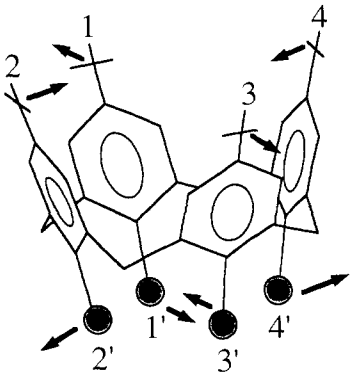

Figure 2. Scheme of the mechanical coupling in calix[4]arenes.

The interaction energies for the cation–ligand (E_{M^+-L}), cation–water (E_{M^+-w}), ligand–water (E_{L-w}), and water–water (E_{w-w}) groups have been calculated from the MD trajectories. The contribution of the ligand L is dissected further into those of its amide and phenolic parts (see Chart I). These energies fluctuate by 0.2–0.8 kcal/mol, except for E_{w-w} and for the total energy of the system (about 4 kcal/mol). Fluctuations on cation–oxygen distances and on $C_t \cdots C_t$ distances are respectively 0.10–0.30 and 0.70–0.80 Å.

Results

I. Calixarene L and Its Complexes *in Vacuo*.

1. The Free Calixarene. The gas-phase dynamics started from the minimized L(C), L(D), and L-free forms. L(D) evolved after a few picoseconds from a C_{4v} to a C_2 symmetry structure with an elongated "ellipsoidal" cone, which did not change during the 300 ps of the simulation. Only slight oscillations of the aromatic fragments took place. The average distances between opposite phenolic oxygens $O_{p1} \cdots O_{p3}$ (3.75 Å) and $O_{p2} \cdots O_{p4}$ (5.88 Å) are close to X-ray data for the uncomplexed tetraamide (3.50 and 5.45 Å).[3] Starting from the L(C) converging structure leads immediately to diverging reorientation of the carbonyls and to a C_{2v} cone. The L-free structure retained a 2-fold symmetry with relaxation of the amide chains.

Because at 300 K the cone itself displayed a low mobility for 300 ps, we ran a 200-ps simulation at 800 K starting from L(D), in order to provide enough kinetic energy to interconvert conformers. Indeed, at this temperature and for the first 50 ps of the simulation, a concerted motion of the cone and of the phenolic oxygens interconverts C_{2v} forms (Figure 2), leading on the average to a C_{4v} cone. The $C_{t1} \cdots C_{t3}$ and $C_{t3} \cdots C_{t4}$ distances oscillate in opposite phase, as do the $O_{p1} \cdots O_{p3}$ and $O_{p2} \cdots O_{p4}$ distances (Figure 3). Figure 3 shows also the coupling between the opening/closing of the cone ($C_{t1} \cdots C_{t3}$) and the pinching of the ether binding sites at the lower rim at 800 K. After 50 ps, the molecule is trapped in a stable form with an elongated C_{2v} cone, without further interconversions.

The minimized L(C) and L(D) forms have similar energies (ΔE = 3 kcal/mol) and are about 35 kcal/mol less stable than the minimized L-free form. However, after MD relaxation at 300 K or at 800 K and minimization, their energy is close to that of L-free. The amide chains adopt different orientations, their cone is highly elongated, and two opposite phenolic oxygens which are very close to each other have amide arms clearly diverging. There are therefore several alternatives to the L-free form for the uncomplexed calixarene *in vacuo*, with no preformed pseudocavity at the lower rim.

In fact, elongated cones are found in several X-ray structures of carbonyl derivatives of calix[4]arenes,[3,10,16,24,49] where the cone is empty, like in the L-free form. Typically, two opposite O–CH_2 groups point inside the pseudocavity, as found in the simulation, with a $CH_2 \cdots CH_2$ distance of about 4 Å. Molecular mechanics calculations by Grootenhuis *et al.*[28] on the tetramethyl ether derivative of *p-tert*-butylcalix[4]arene also find the C_{4v} structure as a saddle point and the cone with only C_{2v} symmetry.

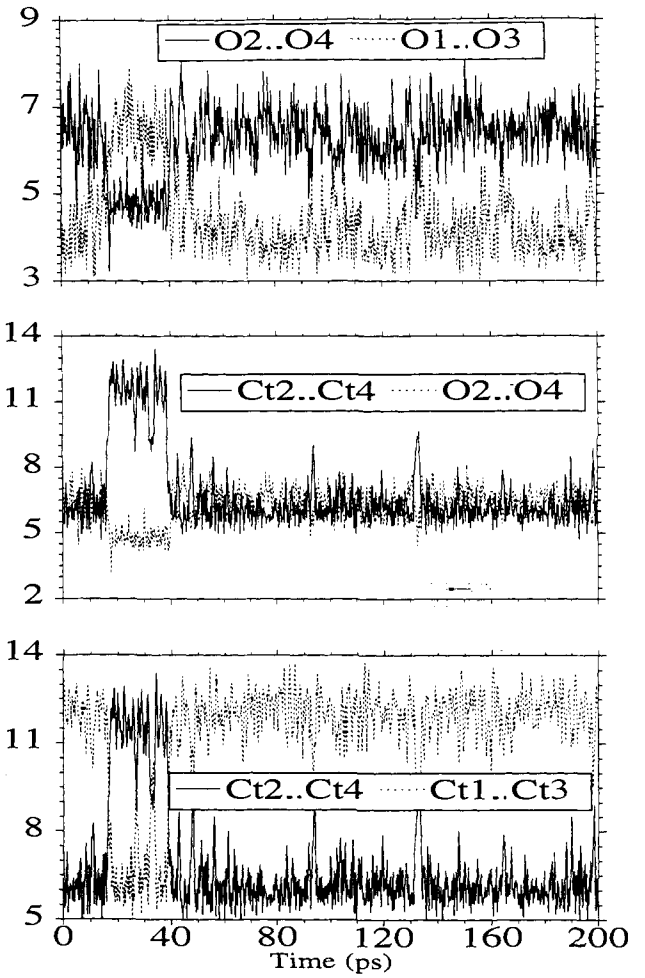

Figure 3. Free calix[4]arenetetraamide at 800 K *in vacuo*. Crossed distances at the upper rim and at the lower rim as a function of time.

We performed an energy component analysis on these structure in order to understand the driving forces for reorganization of 4-fold to 2-fold or lower symmetry structures, based on five groups: the cone and the four amide arms. The cone itself has, in fact, similar energies in these structures, while the interactions of each amide arm with other fragments are always repulsive (about 22 kcal/mol in the L(C) form). Relaxation from axial to equatorial orientations of two opposite amide chains in fact reduces this repulsion. The cone's shape therefore follows rather than drives the structure at the lower rim.

2. The Complexes of L with Alkali Cations (Li^+–Cs^+). In the gas phase, for a given cation, the average structures of the LM^+ complexes after 50 ps are independent of the starting form. Both converging (L(C)) and diverging (L(D)) initial structures lead to converging carbonyls, *i.e.*, to 4/0 complexes. The only exception is LLi^+, which is of either 3/1 or 4/0 type, depending on the starting structure. However, significant perturbations are observed as a function of the cationic size (see Table II and Figure 4). In particular, as the size of M^+ increases, the carbonyls move from "linear" to "tangential" contacts with M^+, *i.e.*, the $M^+ \cdots O{=}C$ angles change schematically from 0° to 90° (Figure 4).

In the 3/1 Li^+ complex, the cation sits away from the symmetry axis, closer to the C=O than to the ether oxygens, coordinated only to one O_p and three carbonyls. The phenolic oxygens outline a parallelogram, with diagonal distances of 3.74 and 5.97 Å, and the cone remains elongated due to the asymmetry of the pseudocavity. The 4/0 complex has the same energy, since its

(49) Arduini, A.; Pochini, A.; Reverberi, S.; Ungaro, R.; Andreetti, G. D.; Ugozzoli, F. *Tetrahedron* **1986**, *42*, 2089–2100.

Table II. Complexes of L with Cations in the Gas Phase: Structural and Energy Characteristics (averaged from MD simulations)[a]

	Li^+	Na^+	K^+	Cs^+
E_{M^+-L}[b]	186.1	162.9	132.1	103.5
$\%E_{M^+-L(a)}$[c]	66	46	42	45
$-E_{LM^+}$[d]	347.3	324.1	297.8	275.5
$M^+\cdots(O_p)$[e]	1.91	1.25	1.43	2.04
$M^+\cdots O_p$[f]	2.04 3.60–5.50	2.62–2.67	2.89–2.90	3.28–3.52
$M^+\cdots O_a$[g]	1.74–1.79 6.23	2.50–2.58	2.81–2.87	3.26–3.31
$O_p\cdots O_p$[h]	3.74–5.97	4.67	5.02	5.32

[a] All energies in kcal/mol; distances in angstroms. [b] Cation–ligand interaction energy. [c] Contribution of the amidic part of L to E_{M^+-L}. [d] Total energy of the complex. [e–h] Averaged distances between M^+ and phenolic (*f*) or amidic (*g*) oxygens, between M^+ and the plane of phenolic oxygens (*e*), or between 1,3- and 2,4-phenolic oxygens (*h*).

better ion–ligand interactions are compensated by enhanced amide–amide repulsions.

The Na^+, K^+, and Cs^+ cations are encapsulated by the four phenolic and four amide oxygens of L, which make two parallel planes. Phenolic oxygens there form a square, whose average size increases with the diameter of the cation (4.67, 5.00, and 5.32 Å for Na^+, K^+, and Cs^+, respectively).

The minimized and MD average geometries of LK^+ are very close to the experimental one. The minimized distances $K^+\cdots O_a$ (2.75 Å) and $K^+\cdots O_p$ (2.85 Å) coincide with the experimental ones within 0.1 Å, and $O_{p1}\cdots O_{p3}$ and $O_{p2}\cdots O_{p4}$ (4.90 Å) within 0.2 Å. The average ⟨MD⟩ distances are about 0.10 Å larger than the minimized ones.

Concerning the motions in the LM^+ complexes, the aromatic fragments display large oscillations, but the lower rim is made rigid by the cation (Figure 5). In contrast to what was found for the free host at 800 K (Figure 3), there is thus no dynamical top–bottom coupling. The cone of the Na^+, K^+, and Cs^+ complexes undergoes several interconversions between C_{2v} forms, which are, however, less elongated than in the free host. The $C_{t1}\cdots C_{t3}$ and $C_{t2}\cdots C_{t4}$ distances are anticorrelated and, in addition to short fluctuations, oscillate by about 5 Å during the cone's transformations (Figure 5). Like LK^+ in the solid state, these complexes adopt on the average a C_{4v} symmetry because of interconversion of the C_{2v} cones and the 4-fold arrangement at the pseudocavity.

3. Complexes with a Neutral Guest Molecule (H_2O, MeCN, MeOH) inside the Cone.

Complex of L with Acetonitrile. The simulations were performed with two starting orientations for MeCN: the methyl group pointed either inside or outside the cone of the L(D) conformer. Both simulations led to a similar complex, with the host–guest interaction energy of –22.2 kcal/mol and acetonitrile's methyl group directed inside the cone, which retains on the average its 4-fold symmetry. The guest is tilted from the C_4 axis and rotates irregularly along that axis (Figure 6). On the average, its position coincides with the symmetry axis, like in the X-ray structure of its complex with *p-tert*-butylcalix[4]-arenetetracarbonate.[24]

The MeCN guest fits nicely inside the cone and reduces its conformational freedom. It also lowers the kinetic barrier between C_{2v} forms, leading to an average C_{4v} cone at 300 K. The plot of distances between MeCN and benzene moieties (Figure 7) illustrates this motion. Upon rotation, the guest seems to "push" aromatic rings of L which oscillate regularly. There is therefore a coupling between the motion of the guest and the pseudorotation of the cone.

Complex of L with Methanol. At the beginning of the dynamics, the methyl group of MeOH pointed inside the cone and the OH pointed outside. During the simulation, MeOH reorients with its oxygen lone pairs pointing outside the cone and the H–O bond and methyl groups more or less perpendicular to opposed aromatic rings (Figure 6). The guest rotates around the symmetry axis. The average symmetry of the host is C_4, and that of the cone is C_{4v}. The host–guest interaction energy is –11.0 kcal/mol, *i.e.*, half that of the MeCN·L complex.

Complex of L with H_2O. In the starting configuration, the water molecule was oriented with its oxygen atom O_w pointing inside the cone, but during the dynamics a complete reorientation occurred. After 300 ps, the O_w atom sits outside the cone (1.06 Å below the plane of central *tert-butyl* carbons), whereas the water protons H_w are directed to the centers of two opposite aromatic rings of L, which are roughly parallel (Figure 6). The water molecule lies perpendicular to the plane of methylene bridging carbons. As a result, the cone keeps a very elongated C_{2v} form along the simulation, without interconversions. The average "diagonal" $C_t\cdots C_t$ distances are 11.85 and 6.67 Å, and the $O_p\cdots O_p$ distances are 3.54 and 6.16 Å. The average distances between O_w and the center of aromatic rings are 3.84 and 4.06 Å for the 1,3 pair and 3.16 and 3.14 Å for the 2,4 pair. The latter are in good agreement both with experimental (3.35 Å) and calculated *ab initio* values (3.19 Å) for the 1:1 benzene–water dimer.[50] The host–guest interaction energy is –10.4 kcal/mol, where electrostatic contribution is more than 80%.

4. Na^+ Complexes of Calixarene with a Guest Inside the Cone. The simulations of the complexes of L with two guests (Na^+ in the polar pseudocavity and S (S = H_2O, MeOH, MeCN)) inside the cone were performed from both L(C) and L(D) starting conformations of the ligand. The guest S had initially its negatively charged atom oriented toward Na^+ in order to provide optimal $S\cdots Na^+$ interactions. This turned out to be unstable, and S rotated to a similar position as in the above LS complexes. Analysis of the energy components before and after this guest's reorientation (Table III) shows that the guest's orientation is in fact determined by its interactions with the cone rather than with Na^+.

Starting from the L(D) form 0/4, the diverging carbonyls converge to Na^+, which in turn moves away from both the phenolic oxygens and S. Accordingly, the distance between Na^+ and the plane of phenolic oxygens increases from 0.2–0.4 to 1.15–1.43 Å. The "lifetime" of the starting $Na^+\cdots S$ coordination correlates nicely with Na^+—S interaction energy (Table III): 15 (MeOH), 35 (H_2O), and 190 ps (MeCN). All final structures are of 4/0 type, and the guest has a similar position as in the LS complexes without cation. The only difference is found in the LNa^+H_2O complex, where water protons bridge either opposite aromatic fragments or neighboring ones as well. In all LNa^+S complexes, the cone is nearly 4-fold symmetric and the Na^+–S interactions are repulsive.

Interestingly, starting the dynamics with the L(C) 4/0 structure and MeCN inside the cone (methyl pointing outside) leads to the decomplexation of MeCN. This results from the repulsion of MeCN with the cone and the too-weak attractions with the remote Na^+. In the simulation starting from L(D), the starting $Na^+\cdots S$ distance was shorter, and step-by-step reorientation of S inside the cone could take place.

Replacement of a neutral guest by SCN^- in the cone leads to a dramatic transformation, due to the strong $M^+\cdots SCN^-$ attraction. During the dynamics of the LM^+SCN^- complexes (M^+ = Li^+–K^+), M^+ loses its carbonyl coordinations and is pulled inside the cone to form an "intimate" $M^+\cdots SCN^-$ ion pair. Only Cs^+, too big to move inside the cone, remains in the pseudocavity.

II. The Calixarene L and Its M^{n+} Complexes in Water. In water, the picture of the calixarene L and of its cation complexes is very different both from the one of the K^+ complex in the solid state and from the structures simulated *in vacuo*. The solvent

(50) Suzuki, S.; Green, P. G.; Bumgarner, R. E.; Dasgupta, S.; Goddard, W. A., III; Blake, G. A. *Science* **1992**, *257*, 942–945.

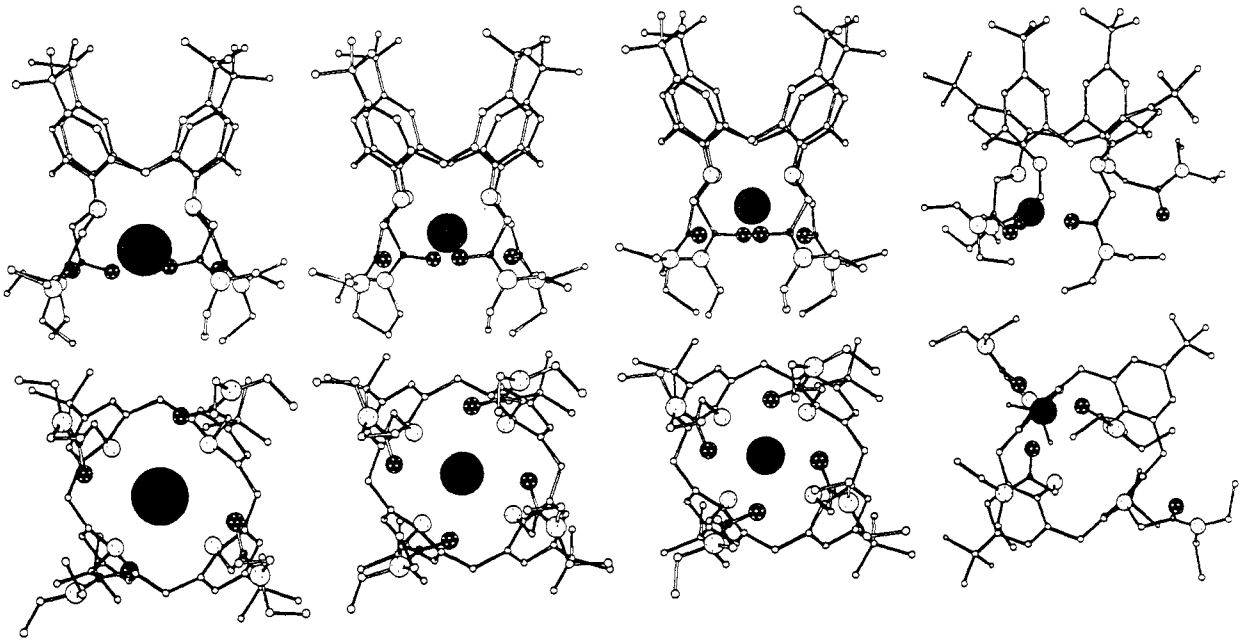

Figure 4. Orthogonal views of the Cs^+, K^+, Na^+, and Li^+ complexes of calix[4]arenetetraamide *in vacuo* (structures minimized after 50 ps of MD).

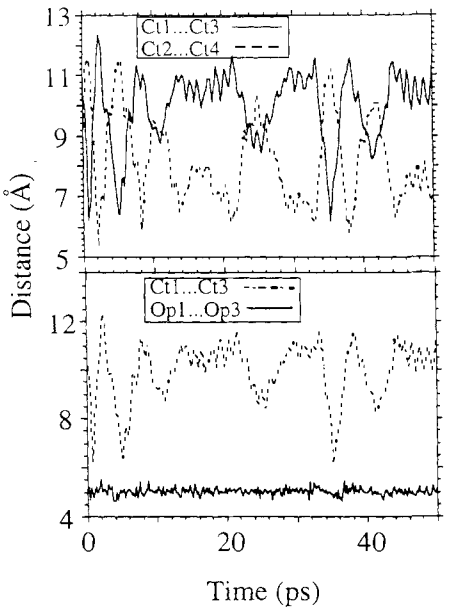

Figure 5. Complex LK^+ *in vacuo*. Crossed distances $C_{t1}\cdots C_{t3}$, $C_{t2}\cdots C_{t4}$ (top) and $C_{t1}\cdots C_{t3}$, $O_{p1}\cdots O_{p3}$ (bottom) are shown as a function of time.

can interact significantly with the cation and the amide groups when the pseudocavity opens. In all simulations starting with 4/0 converging carbonyls, conformational transitions take place at the lower rim. Typical coordination patterns of the cation are shown schematically in Figure 8. The lifetime of the starting L(C) structure (170 ps for Li^+, 100 ps for Na^+ and K^+, 3 ps for Cs^+) follows roughly the order of cation–calixarene interactions energies *in vacuo*. When there is no cation, the pseudocavity opens immediately. The energy component analysis (Tables IV–VIII) shows that the driving forces for reorganization of the LM^+ complexes are the enhanced hydration energy and the ligand stability, while the cation–ligand interactions decrease. Other components (*e.g.*, the water–water energy) may vary as well, in a nonsystematic manner.

In the initial L(C) forms, the cation is completely shielded from water. There is no peak in the ion–water rdf, and M^+ has repulsive interactions with water. After partial opening of the pseudocavity, the cation moves slightly toward the solvent and is coordinated to water molecules. The characteristics of the first-shell hydration of the ion in these partially open forms are reported in Table IX.

In the simulations starting with an open cavity, (*i.e.*, L(D) form) the cation sits closer to the ether than to the diverging carbonyl oxygens, which are hydrated as in free amides. One of the carbonyls then becomes partially converging, leading to a 1/3 form. In the case of LEu^{3+}, the attraction with the ligand is not strong enough to compete with the hydration of Eu^{3+}, and the open complex dissociates rapidly.

We refrain from describing in detail the time evolution of the structures, which are also cation-dependent. Tables IV–VIII summarize average coordination features of the cation to L (distances with carbonyl and ether oxygens) and the energy components of the system. In the following sections, some specific features of the free calixarene and of its complexes are described.

1. The Free Calixarene L. As was done in the gas phase, three forms of the free calixarene were considered in water: L(D), L(C), and L-free.

During 50 ps of MD, the L(D) calixarene keeps its diverging orientation of the carbonyl groups, as observed *in vacuo*. All carbonyls are well hydrated and display only small motions. Each of them is hydrogen-bonded to about two water protons, giving rise to a pronounced peak at 1.90 Å in the O_a–H_w rdf. Such hydration patterns are similar to those calculated for free *N*-methylacetamide and dimethylformamide,[51] indicating the accessibility to water at the lower rim in this diverging form.

The L-free form is metastable in water and adopts after 20 ps a more open lower rim, like in the model-built L(D) form, with four equatorial amide arms, and has similar hydration features.

The L(C) form with a pseudocavity is unstable in water as *in vacuo* and becomes partially diverging in the first picosecond of the simulation. Weak constraints (k = 5 kcal/Å) on all atoms were necessary to maintain this "organized" structure. An energy component analysis shows that its instability results from the amide–amide repulsions (about 20 kcal/mol per group) rather than from a solvation effect. In fact, among the three forms of L considered, L(C) is the best hydrated. Upon opening, the ligand stabilizes by about 70 kcal/mol, *i.e.*, about twice the loss in hydration energy.

(51) Jorgensen, W. L.; Swenson, C. J. *J. Am. Chem. Soc.* **1985**, *107*, 1489–1496.

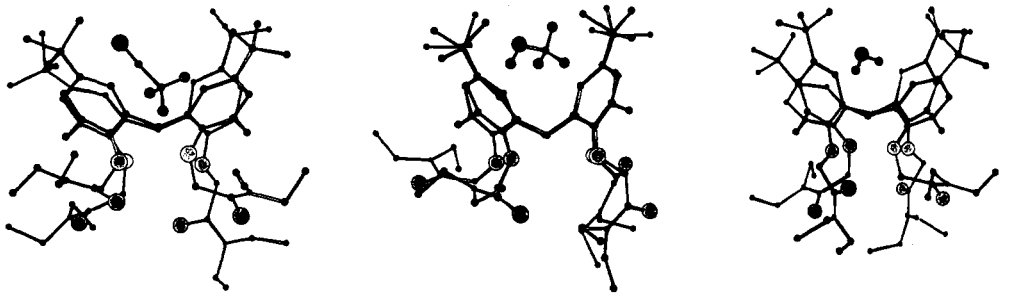

Figure 6. Structures of the complexes of calix[4]arenetetraamide with MeCN (left), MeOH (middle), and H_2O (right) *in vacuo*.

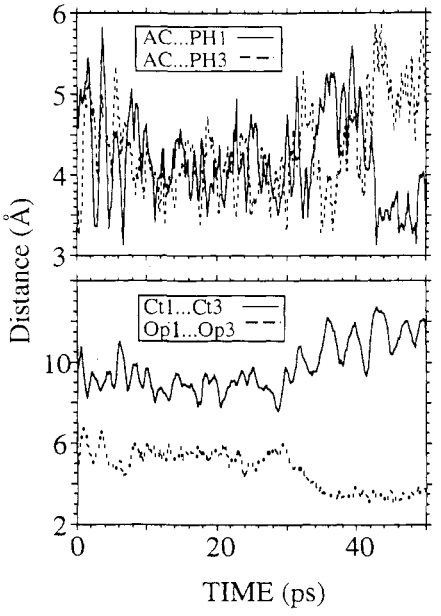

Figure 7. Complex of calix[4]arenetetraamide with MeCN *in vacuo*. The distance between the center of mass of MeCN (AC) and of the aromatic fragments (PH1 and PH3) of the ligand (top) and crossed distances $C_{t1}\cdots C_{t3}$ and $O_{p1}\cdots O_{p3}$ (bottom) as a function of time.

The cone of the three forms is C_{2v} and elongated, without water inside. This is somewhat surprising, given that the affinity calculated above for one water molecule and the cone (−10.4 kcal/mol) is similar to the average energy of one water molecule in the bulk solvent. There is likely a kinetic barrier due to the hydrophobic gate of the four tBu groups which is not overcome during the 50 ps.

2. The LM^{n+} Cation Complexes. The Complex LLi^+. During the first 170 ps starting from L(C), Li^+ remains coordinated in LLi^+ as *in vacuo* by one phenolic and three carbonyl oxygens (conformer **1**; see Figure 8). At 170 ps, a conformational transition (conformer **1** → conformer **2**) takes place due to a repositioning of the cation (Figures 8 and 9), which moves "below" the plane of three amide oxygens and away from the O_p plane (from 1.78 to 3.30 Å). Accordingly, Li^+ is less attracted by L but interacts better with water in conformer **2** than in conformer **1** (Figure 9). In both conformers the amide oxygens coordinated to Li^+ are much less hydrated than in the other complexes, which form about two hydrogen bonds with water protons like in free ligand L (Figure 10).

The Complex LNa^+. The 4/0 LNa^+ rather complex retains its starting L(C) conformation for the first 100 ps of the simulation in water. One of the amide oxygens then turns out to the solvent, followed 30 ps later by a second one, making respectively 3/1 and 2/2 structures (Figure 8). The interaction energy and distances between Na^+ and phenolic oxygens remain almost constant during the simulation, close to the corresponding *in vacuo* values (Table V). The distances between Na^+ and the C=O oxygens which are converging are also nearly identical for all conformers, and the total cation–ligand interaction energy decreases with the number of coordinated carbonyls. In all conformers, a correlated motion of 1,3- and 2,4-*tert*-butyl groups with interconversion of C_{2v} forms of the cone leads to an average C_{4v} cone.

The cation–water and ligand–water interaction energies change as expected in the series 4/0, 3/1, 2/2 (Table V). During the 3/1 → 2/2 transformation, one water molecule coordinates to Na^+.

The Complex LK^+. LK^+ is more flexible than the LNa^+ or LLi^+ complexes and undergoes several conformational transitions in water, which are schematized in Figure 11. Between 100 and 260 ps, the starting 4/0 LK^+ structure evolves to 3/1, 2/2, and 1/3 types. The lifetimes range from 8 to 55 ps. Interconversions result from a compensation of cation–water E_{M^+-w} and cation–ligand E_{M^+-L} interaction energies which are anticorrelated (Figure 13 and Table VI). Typical hydration patterns are shown in Figures 12 and 15.

The Complex LCs^+. The 4/0 cesium complex becomes 3/1 in a few picoseconds and 1/3 after 40 ps: three amide oxygens leave the cation and move to water. After an additional 70 ps, another transition (1/3 → 2/2) takes place, and no other conformer appears during the remaining 90 ps of the simulation. In all these forms, Cs^+ keeps the same "altitude" over the phenolic oxygens and a nearly constant interaction energy with the phenolic part of the ligand (Table VII).

The Complex LEu^{3+}. During the first 25 ps (conformer **1**), Eu^{3+} is coordinated to all oxygens of the ligand and lies between the parallel planes of O_p and O_a atoms. It is completely shielded from water. After 25 ps, a conformational transition (conformer **2**) similar to that observed with Li^+ occurs. However, unlike Li^+, Eu^{3+} sits on the average on the symmetry axis of L and below the plane of four O_a atoms, *i.e.*, it has moved from the pseudocavity to the solvent (Figure 14). A first peak at 2.3 Å in the $Eu^{3+}\cdots O_w$ rdf integrates to about four water oxygens in the first shell of Eu^{3+}. One of them is anchored inside the calixarene by two hydrogen-bonded phenolic oxygens and by Eu^{3+}.

The transition from conformer **1** to conformer **2** corresponds to an important destabilization of the solute (about 80 kcal/mol), which is more than compensated for by larger interactions with water (of about 200 kcal/mol, with a contribution of 240 kcal/mol from Eu^{3+} itself). The water–water interaction energy is almost unchanged (Table VIII). Thus, unlike LLi^+, where several conformers are in equilibrium, the Eu^{3+} complex evolves from a metastable form to a more stable form in water.

3. General Features of Hydration.

The Hydrophilic Part of the Complexes. The hydration pattern of the amide part of the calixarene complexes depends on the size and charge of the cation and on the conformation of the amide moieties.

In the fully converging 4/0 conformers of the Na^+ and K^+ complexes and conformer **1** of LLi^+, the cation is completely encapsulated and prevented from direct coordination to water. Its interactions with water are repulsive (Tables V and VI).

Concerning the carbonyl groups, no tight hydration shell is observed for the forms conformer **1** of LLi^+ and 4/0 of LNa^+.

Table III. Structural and Energy Characteristics of the LNa^+S Complexes in Vacuo before and after the Structural Reorganization[a]

		MeOH		H_2O		MeCN		SCN^-
parameter	no guest	before	after	before	after	before	after	before
$-E_{M^+-L}$	162.9	107.0	163.7	99.7	165.4	120.9	163.7	75.8
$-E_{L-S}$[b]		0.2	11.5	-4.5	10.3	-17.6	25.5	-15.4
$-E_{M^+-S}$[c]		14.8	-2.3	19.7	-4.0	32.1	-11.7	114.2
$-E_{LM^+}$	324.1	315.2	331.7	314.4	327.4	327.0	334.6	372.5
$M^+\cdots(O_p)$	1.25	0.40	1.31	0.35	1.15	0.22	1.43	0.99
$M^+\cdots X$[d]		2.80	6.30	2.51	5.50	2.52	8.00	2.33

[a] Average MD results; energies and distances are defined in Table II. [b,c] Interaction energy between the guest S and the ligand (*b*) or the cation (*c*). [d] Distance between the cation and the X atom of S (X = O for MeOH and H_2O; X = N for MeCN and SCN^-).

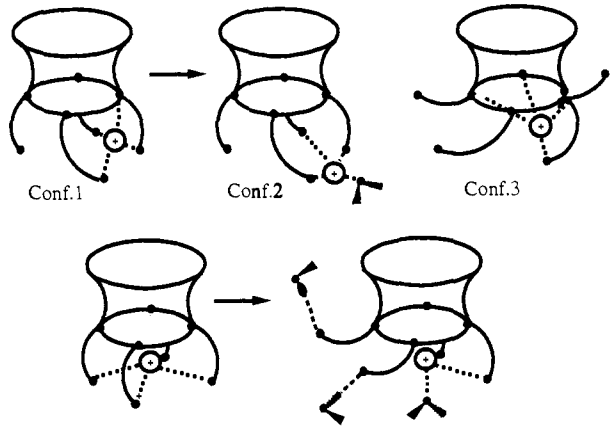

Figure 8. Schematical representation of cations' binding modes in water. The three conformers of LLi^+ (top) and the **4/0** and **2/2** conformers of Na^+, K^+, and Cs^+ complexes of calix[4]arenetetraamide (bottom) are shown.

Table IV. Structural and Energy Characteristics of the LLi^+ Complex in Water[a]

parameter	conformer **1**	conformer **2**	conformer **3**[i]
N_w[b]	1031	1031	997
lifetime (ps)	0–170	170–250	0–70
$-E_{tot}$[c]	8657.5	8652.5	8640.9[j]
$-E_{w-w}$[d]	8169.9	8164.5	8157.2[j]
$-E_{M^+-L}$	188.6	168.4	134.3
$\%E_{M^+-L(a)}$	62	74	14
$-E_{LM^+}$	393.3	376.0	360.8
$-E_{M^+-w}$[e]	4.6	36.7	3.7
$-E_{L-w}$[f]	90.8	75.3	119.3
$\%E_{L(a)-w}$[h]	48	43	64
$-E_{LM^+-w}$[g]	95.4	112.0	123.0
$M^+\cdots(O_p)$	1.78	3.30	0.44
$M^+\cdots O_p$	2.26 3.18–4.95	3.37–4.74	1.95–2.48
$M^+\cdots O_a$	1.75–1.82 7.02	1.77–1.79 7.88	1.78 5.01–5.75

[a] Average MD results; see Table II for definitions of E_{M^+-L}, $\%E_{M^+-L(a)}$, E_{LM^+}, $M^+\cdots(O_p)$, $M^+\cdots O_p$, and $M^+\cdots O_a$. [b] Number of water molecules in the simulation box. [c] Total energy of the simulation box. [d] Water–water energy in the simulation box. [e–g] Interaction energy between water and the cation (*e*), water and the ligand (*f*), and water and the complex (*g*). [h] Contribution of the amidic part of L to the hydration energy of the ligand. [i] Simulation starting from the L(D) form. [j] Renormalized to 1031 water molecules.

This contrasts with the 4/0 LK^+ and 3/1 LNa^+ complexes, where the carbonyls have suitable distances and orientations to be bridged by hydrogen-bonded water molecules. In LK^+ (Figure 12), two water molecules "bridge" two pairs of adjacent carbonyls (–22 kcal/mol), which largely compensates for the $K^+\cdots$water repulsion (+11 kcal/mol). Like in cation cryptates simulated in water,[27] there is a "negative cooperativity" between solvation of the complexed ion and its binding sites. Such bridging pattern are similar to those found with macrocyclic compounds in the solid state[52,53] and by computer simulations.[54,55]

Table V. Structural and Energy Characteristics of the LNa^+ Complex in Water[a]

	i/*j*[b]			
parameter	4/0	3/1	2/2	1/3[c]
n_w	995	995	995	1021
lifetime (ps)	0–100	100–130	130–300	0–70
$-E_{tot}$	8298.8	8330.8	8370.2	8323.2[d]
$-E_{w-w}$	7848.5	7865.5	7926.4	7863.5[d]
$-E_{M^+-L}$	163.6	153.0	124.6	94.7
$\%E_{M^+-L(a)}$	45	41	33	11
$-E_{LM^+}$	370.3	335.9	339.1	330.0
$-E_{M^+-w}$	-2.7	-19.3	10.8	19.1
$-E_{L-w}$	82.6	134.8	93.9	110.7
$\%E_{L(a)-w}$	42	52	53	64
$-E_{M^+L-w}$	79.9	115.7	104.7	129.8
$M^+\cdots(O_p)$	1.25	1.04	1.08	0.70
$M^+\cdots O_p$	2.63–2.68	2.54–2.61	2.57–2.75	2.51–2.61
$M^+\cdots O_a$	2.50–2.54	2.46–2.54 4.48	2.44–2.47 4.61–4.69	2.49 4.46–5.87

[a] See Tables III and IV for definitions. [b] Converging/diverging carbonyls. [c] Simulation starting from L(D) form. [d] Renormalized to 995 water molecules.

Table VI. Structural and Energy Characteristics of the LK^+ Complex in Water[a]

	i/*j*		
parameter	4/0	open-type conformers	1/3[b]
N_w	1018	1018	997
lifetime (ps)	0–100	100–260	0–70
$-E_{tot}$	8496.9	8499.3	8489.6[c]
$-E_{w-w}$	8058.7	8058.3	8054.1[c]
$-E_{M^+-L}$	136.1	103.1	86.6
$\%E_{M^+-L(a)}$	44	33	18
$-E_{LM^+}$	328.5	316.4	309.6
$-E_{M^+-w}$	-19.7	7.1	14.0
$-E_{L-w}$	129.3	117.5	111.9
$\%E_{L(a)-w}$	58	61	61
$-E_{ML^+-w}$	109.7	124.6	125.9
$M^+\cdots(O_p)$	1.37	1.38	1.19
$M^+\cdots O_p$	2.89–2.93	2.89–2.97	2.86–2.91
$M^+\cdots O_a$	2.91–3.00	2.93, 3.23 4.49, 4.67	2.99 3.26–5.87

[a] See Tables II and IV for definitions. [b] Simulation starting from L(D) form. [c] Renormalized to 1018 water molecules.

The 4/0 conformers of LNa^+ and LK^+ complexes can be considered to be isosteric,[100] since the encapsulated cations are shielded from water and their form and size do not differ much. Their solvation energy is, however, very different (–79.9 kcal/mol for LNa^+ and –109.7 kcal/mol LK^+) due to differences of hydration patterns. There is no water tightly bound to the amide oxygens of LNa^+, in contrast to LK^+ (Figure 12).

Since the pseudocavity of complexes 1/3 and 2/2 of LNa^+ and 3/1, 2/2, and 1/3 of LK^+ is more or less open, the cation is coordinated to at least one water molecule (attracted by about 11.1 kcal/mol in the case of K^+). Its interaction with other water molecules is repulsive on the average, but the total cation–water

Table VII. Structural and Energy Characteristics of the LCs^+ Complex in Water[a]

parameter	i/j 3/1	1/3	2/2	1/3[b]
N_w	1121	1121	1121	997
lifetime (ps)	0–40	40–110	110–200	70
$-E_{tot}$	9338.4	9365.1	9380.9	9292.9[c]
$-E_{w-w}$	8911.1	8930.6	8955.9	8851.5[c]
$-E_{M^+-L}$	90.8	73.3	86.4	50.0
$\%E_{M^+-L(a)}$	38	29	36	9
$-E_{LM^+}$	313.2	290.2	293.3	279.5
$-E_{M^+-w}$	4.7	22.1	6.7	38.8
$-E_{L-w}$	109.4	122.2	125.0	123.0
$\%E_{ML^+(a)-w}$	60	66	56	70
$-E_{ML^+-w}$	114.1	144.3	131.7	161.9
$M^+\cdots\langle O_p\rangle$	1.95	1.92	1.98	1.73
$M^+\cdots O_p$	3.23–3.43	3.24–3.54	3.30–3.43	3.22–3.45
$M^+\cdots O_a$	3.30–3.72	3.34	3.19, 3.29	3.20
	4.67	4.54–5.37	3.86, 4.88	6.20–6.50

[a] See Tables II and IV for definitions. [b] Simulation starting from the L(D) form. [c] Renormalized to 1121 water molecules.

Table VIII. Structural and Energy Characteristics of the LEu^{+3} Complex in Water[a]

parameter	conformer **1**	conformer **2**
N_w	995	995
lifetime (ps)	0–25	25–125
$-E_{tot}$	8719.4	8838.1
$-E_{w-w}$	7700.4	7692.3
$-E_{M^+-L}$	583.0	489.4
$\%E_{M^+-L(a)}$	62	75
$-E_{LM^+}$	743.4	662.9
$-E_{M^+-w}$	284.2	543.0
$-E_{L-w}$	−8.6	−60.0
$-E_{ML^+-w}$	275.6	483.0
$M^+\cdots\langle O_p\rangle$	1.22	3.39
$M^+\cdots O_p$	2.50–2.58	4.12–4.27
$M^+\cdots O_a$	2.15–2.16	2.23, 2.23
		2.24, 2.54

[a] See Tables II and IX for definitions.

Table IX. Analysis of the First Peak of the $M^{n+}\cdots O_w$ and $M^{n+}\cdots H_w$ rdf's for LM^{n+} Complexes in Water Solution

cation	form	$M^{n+}\cdots O_w$ max	$M^{n+}\cdots H_w$ max	hydration number
Li^+	conformer **2**	1.9	2.6	0.32
		4.5	5.1	1.62
Na^+	2/2	2.5	3.2	0.99
	1/3[a]	2.5	3.2	0.72
K^+	open-type	2.9	3.5	1.65
	1/3[a]	2.9	3.5	0.86
Cs^+	2/2	3.3	4.0	5.00
	1/3[a]	3.3	4.0	3.92
Eu^{3+}	conformer **2**	2.3	3.0	4.14
		4.4	5.0	6.32

[a] For L(D) starting structure.

interaction remains attractive. In the case of LCs^+, all conformers are of open type because the large size of Cs^+ prevents its full encapsulation by the ligand. As a result, Cs^+ is more hydrated than the other cations and is surrounded by five water molecules within 3.3 Å in the 1/3 and the 2/2 conformers (Table IX). In this complex, the carbonyl oxygens bound to Cs^+ are too far apart from each other to be bridged by water.

There is no second hydration shell around the cation, except in the *exo* complexes of Li^+ and Eu^{3+} with L. In the other cases,

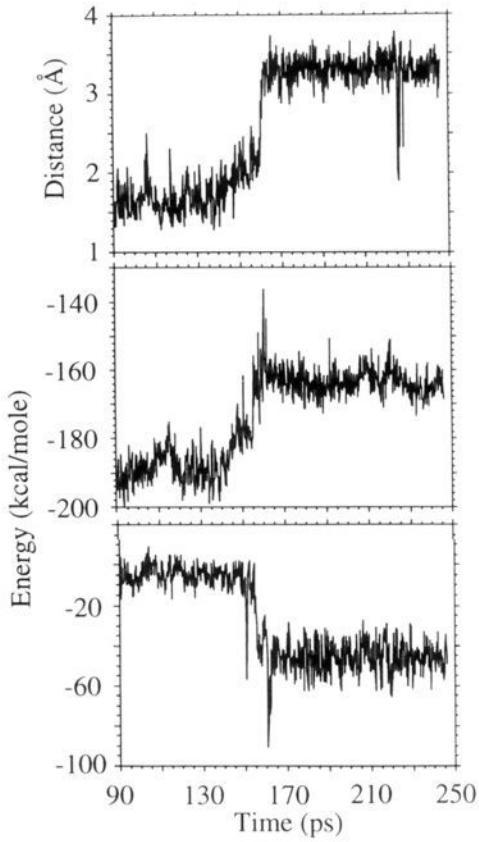

Figure 9. LLi^+ complex in water, from conformer **1** (90–170 ps) to conformer **2** as shown in Figure 8. The distance between Li^+ and the plane of phenolic oxygens (top) and Li^+–ligand (middle) and Li^+–water (bottom) interaction energies are shown as a function of time.

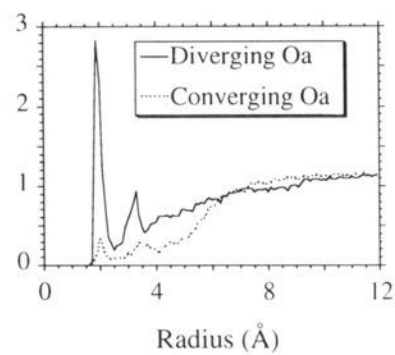

Figure 10. Conformer **2** of the LLi^+ complex in water. The *rdf* $O_1\cdots H_w$ is shown for converging/diverging carbonyls.

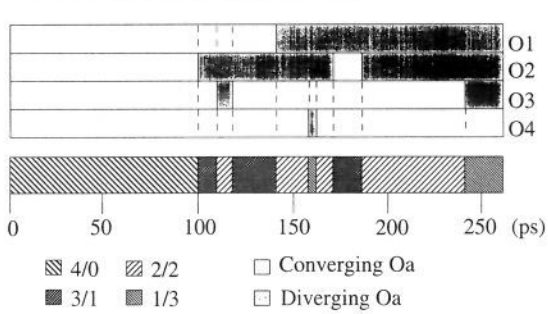

Figure 11. LK^+ complex in water. Scheme of time-dependent converging/diverging orientations of carbonyls (top) and of the resulting conformation of the pseudocavity (bottom).

the water structure beyond 3 Å from the ion results from the calixarene. In the LEu^{3+} complex, we find a water molecule with a particular status. It is, in fact, co-complexed with Eu^{3+} inside

(52) Vögtle, F.; Muller, W. M.; Watson, W. H. *Top. Curr. Chem.* **1984**, *125*, 131–164.
(53) Nordlander, E. H.; Burns, J. H. *Inorg. Chim. Acta* **1986**, *115*, 31–36.
(54) Ranghino, G.; Romano, S.; Lehn, J.-M.; Wipff, G. *J. Am. Chem. Soc.* **1985**, *107*, 7873–7877.
(55) Ben-Naim, A. *Biopolymers* **1990**, *29*, 567–596.

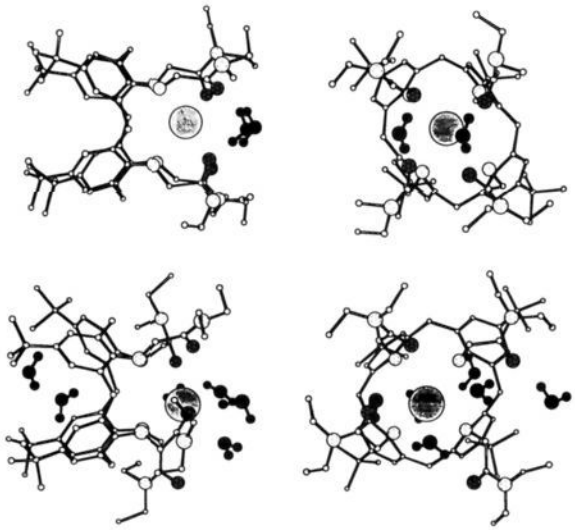

Figure 12. Typical hydration pattern of the **4/0** and **2/2** forms of the LK^+ complex in water.

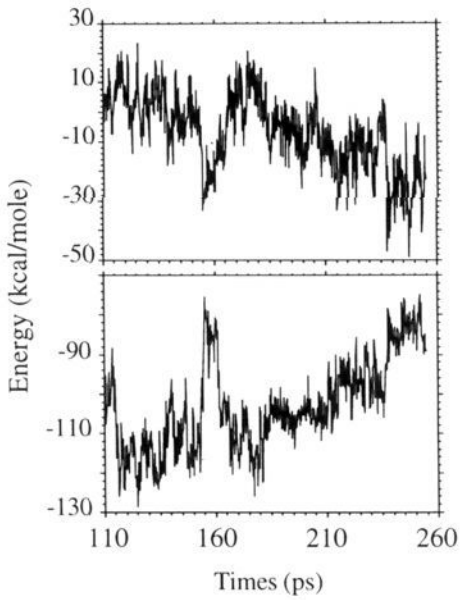

Figure 13. Open-type forms of the LK^+ complex in water. Cation–ligand (top) and cation–water (bottom) interaction energies are shown as a function of time.

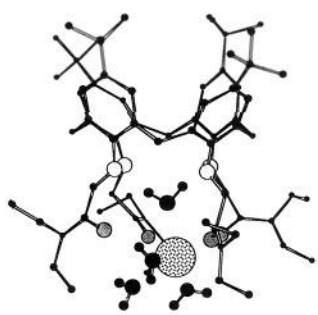

Figure 14. The first hydration shell of Eu^{3+} in the LEu^{3+} complex.

the calixarene, reminiscent of Li^+ and Ca^{2+} 222 cryptates in water, where one water molecule is bound to the cation and doubly hydrogen-bonded to ether oxygens of the cage.[27,121]

Filling the Apolar Cone. The hydration shell of the cones of L and its complexes is typically hydrophobic in terms of solvent structure: first-shell water molecules form a caged network of

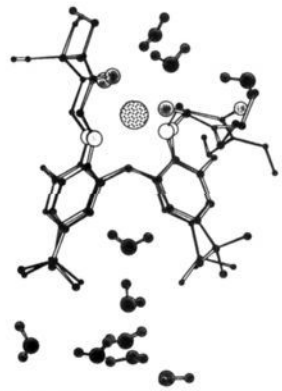

Figure 15. Typical hydration pattern in the cone of the **2/2** LNa^+ and LK^+ complexes.

hydrogen bonds. The most interesting feature is perhaps the "filling of the basket"[2] when some water molecules form a chain which "hangs down" from the dome of the caging water shell into the cone (Figure 15). The deepest water molecule inside the cone occupies almost the same position as simulated *in vacuo* for the LNa^+H_2O complex: O_w points outside, and H_w protons point to the centers of opposite or neighboring aromatic fragments.

Interestingly, the cone is filled by water in some complexes only: LNa^+ (after 110 ps), LK^+ (150 ps), and LCs^+ (100 ps). For other complexes, like LLi^+, there is no water inside, even after 250 ps of MD. For a given complex, the water content of the cone also depends on the conformation at the lower rim. For instance for LNa^+, only the 3/1 and 2/2 forms contain water within 3Å of the center of mass of the four *tert*-butyl groups (Figure 15). The 4/0 cone is empty. The four *tert*-butyls seem therefore to act as a "hydrophobic gate", which can be modulated by conformational changes at the lower rim via the mechanical coupling demonstrated above. This gate controls the kinetic barrier for diffusion of water molecules inside the cone. When sulfonato analogs of calix[4]tetraamide and its complexes are simulated similarly, water moves inside the cone in all cases within 40 ps[56] because of hydrophilic assistance.

In the solid state, water molecules are found in the cone of calix[4]arenes which bear polar, instead of hydrophobic, substituents at the upper rim.[25,57] In all cases the water protons point almost perpendicular to the aromatic planes ("π hydrogen bonding"[25,57,58]), as simulated here.

Although the cone is considered as hydrophobic, it contributes significantly to the hydration energy of the ligand within the LM^+ complexes, like for the free calixarene L (Tables IV–VIII). The cone–water and amide–water interaction energies range respectively from –43 to –55 and from –32 to –81 kcal/mol and depend on M^+ as well as the conformation at the lower rim (Tables IV–VIII). In the conformer **1** or conformer **2** of LLi^+ or the 4/0 form of LNa^+, where carbonyl groups converge "linearly" to the cation, the cone's contribution is more than 50%. In the more open forms, it still contributes up to 35–40% to the calixarene's hydration energy. For the three forms of the uncomplexed ligand L, the cone contributes to about 40% of the total attractions with water (–51 to –54 kcal/mol). In the constrained L(C) form, its contribution is largest (–97 kcal/mol, 51% of the total hydration energy) due to the incorporation of water molecules inside the pseudocavity. The water insolubility of L and LM^+ is therefore expected to result from significant entropic, rather than enthalpic, effects.

The LEu^{3+} complex, which is water soluble, is much more "water attractive" than the LM^+ complexes. It displays a repulsive

(56) Guilbaud, P.; Wipff, G., unpublished results.
(57) Atwood, J. L.; Hamada, F.; Robinson, K. D.; Orr, G. W.; Vincent, R. L. *Nature* **1991**, *349*, 683–694.
(58) Atwood, J. L.; Bott, S. G. In *Calixarenes: a versatile class of macrocyclic compounds*; Vicens, J., Bohmer, V., Eds.; Kluwer Academic Publishers: Dordrecht, The Netherlands, 1991; pp 199–210.

calixarene···water interaction energy, in contrast to the above LM^+ complexes or L which are water insoluble. This repulsion is, however, more than compensated for by a strong Eu^{3+}···water attraction. In the LM^+ complexes, the cation–water interaction was either attractive or repulsive and was small compared to the ligand–water attractions (Tables IV–VIII).

III. Free Energy Perturbation Simulations on LM^+ Complexes in the Gas Phase and in Water. According to the thermodynamic cycle,[43,59–61] the binding selectivity in solution $\Delta\Delta G_c$ for M_1^+ versus M_2^+, measured experimentally by $\Delta G_2 - \Delta G_1$, is equal to $\Delta G_4 - \Delta G_3$, which is more amenable to computer approaches.[44,62–66]

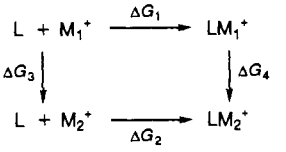

In the gas phase, the relative binding affinities are simply given by ΔG_4, *i.e.*, from the mutation of one complex into the other (Table X). We calculate that the calixarene has intrinsically the highest affinity for the smallest cation Li^+. No peak of selectivity is observed, and the order of intrinsic binding affinities of L is $Li^+ > Na^+ > K^+ > Rb^+ > Cs^+$. These results are consistent with the order of gas-phase interaction energies between alkali cations and ethers or amines[67] and indicate that the ligand is flexible enough to provide an optimal surrounding for each of these ions.

Since L selectively binds Na^+ in methanol and selectively extracts Na^+ from water to dichloromethane or methanol, we paid a particular attention to the Na^+/Li^+ selectivity at a more quantitative level. For the longest simulation (200 ps, 41 windows), the ΔG_4 was 29.7 for the Na^+ to Li^+ mutation and –41.1 kcal/mol for the Li^+ to Na^+ mutation, indicating an important hysteresis. In fact, these mutations involved respectively 4/0 to 4/0 and 3/1 to 4/0 forms. Thus, although the 4/0 and 3/1 forms of LLi^+ have the same minimized energy, they are separated by a kinetic barrier which is not overcome at the beginning of the MD. On the other hand, the LNa^+ complex clearly prefers a 4/0 over 3/1 structure, and starting the Li^+ to Na^+ mutation with the 3/1 form exaggerates ΔG_4, due to the "penalty" suffered by the Li^+–Na^+ hybrid before the four carbonyls begin converging. The ΔG_4 of 29.7 kcal/mol is therefore most appropriate. The other LM^+ complexes remained of 4/0 type, and there was no such hysteresis.

In solution, the stability constants of L with alkali cations have been determined in methanol only, with a marked peak for $Na^+ > K^+ > Li^+ \approx Rb^+ > Cs^+$.[10,11] Since the same peak is found for the ethyl ester, methyl ketone, or acid analogs of the tetraamide L, it is reasonable to assume that the carbonyls display similar coordination features and outline a similar pseudocavity as in L. In acetonitrile, thermodynamic data are available for the ethyl tetraacetate derivative and peak at Li^+, with the sequence $Li^+ > Na^+ > K^+ > Cs^+ > Rb^+$.[11] The same trend is expected for L in acetonitrile.

The relative binding selectivities $\Delta\Delta G_c$ for two ions can be estimated as $\Delta\Delta G_c = \Delta G_{4gas} - \Delta G_{3exp}$, *i.e.*, by correcting the relative intrinsic affinities by the experimental relative desolvation energies of the cations. Such simple procedures imply that the LM^+ complexes are solvated to the same extent and that their structure in solution is close to that *in vacuo*, *i.e.*, of 4/0 type. This hypothesis should hold better in acetonitrile than in methanol, which can interact more strongly with the lower-rim substituents.

In acetonitrile, ΔG_{3exp} for free cations can be calculated from their experimental free energies of transfer (ΔG_t) to water[68] (Table X). For Li^+, for which no data are available, ΔG_t is extrapolated assuming for Li^+ and Na^+ a linear correlation between experimental ΔG_ts from acetonitrile to other solvents.[68,69] This leads to calculated $\Delta\Delta G_c$s which are larger than the experimental values (Table X) but follow almost the same sequence ($Li^+ > Na^+ > K^+ > Rb^+ > Cs^+$) as for ester and ketone analogs of L.[5] The only difference concerns the Cs^+/Rb^+ selectivity, possibly related to partial opening of the pseudocavity by Cs^+, which is not well shielded from the solvent, as seen above in water. The gas-phase structure for its complex is likely to be less relevant than for the smaller cations.

Using the same approach in methanol leads to a peak of selectivity for Li^+, like in acetonitrile, in disagreement with experiment. Since methanol can make hydrogen bonds to the carbonyl oxygens, it is anticipated that the structures of the LM^+ complexes will, like in water, differ from the ones *in vacuo*, and the $\Delta G_{4methanol}$ values should differ significantly from ΔG_{4gas}. Our attempts to compute ΔG_{4water} by mutating the complexes in water

Table X. Relative Free Energies of Mutation (kcal/mol) of Li^+, Na^+, K^+, Rb^+, and Cs^+ Uncomplexed and Complexed by L for Different Simulation Times[a]

	mutations			
	$Li^+ \rightarrow Na^+$	$Na^+ \rightarrow K^+$	$K^+ \rightarrow Rb^+$	$Rb^+ \rightarrow Cs^+$
		ΔG_4		
gas phase				
55 ps	34.5/34.3[b]	20.8	10.4	9.2[d]
	39.6/42.8[c]	21.6[e]		
	31.4/28.8[f,b]			
200 ps	41.3/41.0[c]			
	29.8/29.7[f,b]			
water				
55 ps	29.7/28.0[f]	19.9/19.7		
55 ps[g]	28.8/31.4[f]	18.1/8.0	7.5/7.7	6.9/6.8
105 ps	31.4/31.0[f]		7.5	7.4/7.3[d]
		ΔG_3		
water[h]	23.9	17.6	5.1	7.7
MeCN[i]	18.9	16.2	4.9	7.2
MeOH[j]	23.0	17.0	6.0	9.5
		$\Delta\Delta G_c$ (calculated)		
water				
55 ps[k]	10.5[b]	3.2	5.3	1.5[d]
55 ps[g]	6.9[f]	0.5[e]	2.5	–1.0[d]
55 ps	4.9	2.2		
105 ps	7.3[f]		2.4	–0.3[d]
MeCN[l]	15.5	4.6	5.5	2.0[d]
MeOH[m]	11.4	3.8	4.4	–0.3[d]
		$\Delta\Delta G_c$ (experimental)		
MeCN[n]	0.8	1.8	3.5	–1.2
MeOH[o]	–2.4	1.3	1.2	0.8

[a] Unless specified, the mutation has been performed from the smaller to the larger cation. When two values are given, they correspond to the "forward" and "backward" cumulated energies. When these quantities are equal, only one value is given. [b] 4/0(starting) → 4/0(final). [c] 3/1(starting) → 4/0(final). [d] $Cs^+ \rightarrow Rb^+$ mutation. [e] $K^+ \rightarrow Na^+$ mutation. [f] $Na^+ \rightarrow Li^+$ mutations. [g] Mutation with L(C) starting conformation. [h] Experimental data from ref 120. [i] Calculated using experimental free energies of transfer from refs 68 and 69. [j] Experimental data from ref 28. [k] $\Delta\Delta G_c = \Delta G_4(\text{vacuo}) - \Delta G_3(\text{water})$. [l] $\Delta\Delta G_c = \Delta G_4(\text{vacuo}) - \Delta G_3(\text{MeCN})$. [m] $\Delta\Delta G_c = \Delta G_4(\text{vacuo}) - \Delta G_3(\text{MeOH})$. [n] Experimental data for *p-tert*-butylcalix[4]arenetetraacetate from ref 11. [o] Experimental data for L from ref 13.

(59) Gunsteren, W. F. V.; Berendsen, H. J. *Angew. Chem., Int. Ed. Engl.* **1990**, *29*, 992–1023.
(60) Beveridge, D. L.; DiCapua, F. M. *Annu. Rev. Biophys. Biophys. Chem.* **1989**, *18*, 431–492.
(61) Jorgensen, W. L. *Acc. Chem. Res.* **1989**, *22*, 184–189.
(62) Lybrand, T. P.; McCammon, J. A.; Wipff, G. *Proc. Natl. Acad. Sci. U.S.A.* **1986**, *83*, 833–835.
(63) van Eerden, J.; Harkema, S.; Feil, D. *J. Phys. Chem.* **1988**, *92*, 5076–5079.
(64) Boudon, S.; Wipff, G. *J. Phys. Chem.* **1990**, *94*, 6056–6061.
(65) Grootenhuis, P. D. J.; Kollman, P. A. *J. Am. Chem. Soc.* **1989**, *111*, 2152–2158.
(66) Grootenhuis, P. D. J.; Kollman, P. A. *J. Am. Chem. Soc.* **1989**, *111*, 4046–4051.
(67) Kebarle, P. *Annu. Rev. Phys. Chem.* **1977**, *28*, 445–476.
(68) Gritzner, G. *Pure Appl. Chem.* **1988**, *60*, 1743–1756.
(69) Gritzner, G. *Inorg. Chim. Acta* **1977**, *24*, 5–12.

show that this is not an easy task (see next paragraph). On the other hand, experimental data also show that in methanol the entropy component (ΔS_c) of the complexation energy (ΔG_c) is positive for Li^+ but negative for Na^+,[11] which suggests that more extensive sampling is required to simulate the relative stabilities of these complexes.

Mutations in water (Table X) with different starting structures and simulation times give similar values (within 2 kcal/mol) for the LLi^+/LNa^+ complexes and the same order from LLi^+ to LCs^+ as *in vacuo* (Table X). During the 55 or 105 ps of mutation, the conformation remains close to the starting one, *i.e.*, either of L(C) or L(D) type. Although the cation is better hydrated in the L(D) than in the L(C) forms, the ΔG_4s are similar. All ΔG_4 energies are larger than the corresponding differences in hydration ΔG_3 free energies. As a result, one would again predict the same binding selectivity sequence as in acetonitrile or methanol.

As shown for the mutations *in vacuo*, the question of thermodynamic equilibrium at each step of the mutation is unclear, and the system may remain trapped in regions of the conformational space which are not optimal for initial and final states. In cases of crown ethers,[63,70,71] cryptands,[72,73] valinomycin,[44] nonactine,[74] and related ionophores,[62] which involve organized macro(poly)cyclic ligands, this problem of sampling may not be as severe as with functionalized calixarenes like L, because here many open structures are likely to contribute to the stability of the complex with partial encapsulation of the guest. With crown ether complexes and cryptates, the ligand may adopt several conformations which retain convergent orientations of the binding sites. More extensive sampling, which requires computer means beyond our present capabilities, is required to further investigate this question.

IV. Discussion.

1. Gas-Phase and Solid-State Versus Solution Structure of L and Its Complexes. The structures obtained computationally *in vacuo* for the calixarene L-free and for its LK^+ complex agree nicely with the solid-state structures.[3] For the other cation complexes, no experimental structures are available. According to the calculations in the gas phase, the Na^+, K^+, and Cs^+ cations coordinate all ligand oxygens also to form a 4/0 conformer, while Li^+ may oscillate between the 4/0 and 3/1 forms.

The situation in water is very different from that in the gas phase and in the solid state. The competition between cation–ligand, cation–water, ligand–water, and water–water interactions leads to conformational transformations of the LM^{n+} complexes. Around hard cations (Li^+, Eu^{3+}), the phenolic binding sites are substituted by water molecules and the $M^+\cdots O{=}C$ interactions are retained. The Li^+ cation prefers a tetrahedral coordination to the binding sites of L, both in the gas phase and in water, as in other complexes.[75] The tetrahedron can be formed by one O_p and three O_a atoms (conformer **1**), by three O_a atoms and one water oxygen (conformer **2**), or by one O_a and three O_p atoms (conformer **3**).

For the Na^+, K^+, and Cs^+ complexes, other transformations take place in water. The cation remains coordinated to the phenolic oxygens, but some amide oxygens are replaced by water in its first coordination sphere.

The comparison of structures obtained with different starting conformers suggests that in water, simulation times of a few hundred picoseconds are too small to reach a thermodynamic equilibrium since the L(C) and L(D) starting forms do not converge to the same conformers. Other computer experiments may lead to new conformers. For instance, starting with the 1/3 conformer of the LNa^+H_2O complex (with the H_2O molecule set inside the cone, "coordinated" to Na^+) led to a $1/3 \rightarrow 0/4$ transition in water. The lifetime of one conformer may be very sensitive to the precise starting conformation. For instance, the 4/0 form of LK^+ ($\chi_2 = 150°$, $\chi_3 = 30°$) has a lifetime of 100 ps. Slight changes of the torsional angles ($\chi_2 = 180°$, $\chi_3 = 0°$) lead to the $4/0 \rightarrow 3/1$ conversion within 3 ps, because the C=O dipoles lose their optimal rearrangement.

No firm conclusion can be drawn, therefore, concerning *the* most stable form of the LM^+ complexes in water, and we suggest rather an equilibrium between several forms. The total energy of the simulated box is nearly constant for all alkali cation complexes. In the case of LEu^{3+}, the starting 4/0 form is metastable and evolves to a more stable one with one H_2O molecule co-complexed with Eu^{3+}.

2. Modulation of Complexation Properties at the Lower Rim by Hinge-Like Motions of the Cone: Top–Bottom Coupling. We have described in detail the hinge-like motions of the aromatic fragments around the (meta)$CH_2\cdots$(meta)CH_2 axis of the cone, as schematized in Figure 2, where top–top, bottom–bottom, and top–bottom couplings can all take place. Taking advantage of such top–bottom coupling may relate structural changes of one moiety (*e.g.*, the top) and the binding capability at a remote site (*e.g.*, the bottom). Perturbations may be provided by the complexation of one guest or from chemical modifications. For instance, in the LLi^+ complex, rigidness of the hydrophilic part leads to the most asymmetrical cone, where two opposite *tert*-butyl groups are on the average much closer (5.7 Å) than in the other LM^+ complexes (9.5–9.7 Å). This may explain why no water molecule diffuses into the cone of LLi^+, in contrast to the Na^+, K^+, and Cs^+ complexes. On the other hand, one water molecule, which was set initially inside the cone of the LLi^+ complex, remained at the same position for 300 ps in water, as simulated *in vacuo*. In this case, cone deformations induced at the lower rim[77] increase the kinetic barrier for (de)complexation of neutral guests.

Interestingly, calixarene derivatives with 1,3 aromatic fragments bridged by an alkyl chain $(CH_2)_n$ form less stable complexes as n decreases.[78] The small distance between 1,3 fragments imposed by the bridge induces a (too) large distance between 1′,3′ phenolic oxygens and prevents optimal arrangement of the pseudocavity. Taking advantage of this top–bottom coupling might lead to the design of pH-switched cation receptors based on calixarenes. For instance, 1,3 aromatic fragments of the cone, substituted respectively by one proton donor and one acceptor group, could be bridged via hydrogen bonding. The pH modulation of this cross-link could open/close the cone and decomplex/complex the cation at the lower rim.

3. The Question of Molecular Preorganization. The uncomplexed calixarene L has no preformed cavity at the lower rim to complex a cation in the solid state, in the gas phase, or in water. The repulsion between binding sites prevents such a preorganization in L and presumably in calixarene analogs containing oxamide, thioamide, phosphate, and tosylate groups.[79,80] The energy price to organize pseudocavities, an important contribution of the polymacrocyclic effect,[81–85] has to be more than compen-

(70) Mazor, M. H.; McCammon, J. A.; Lybrand, T. P. *J. Am. Chem. Soc.* **1989**, *111*, 55–56.
(71) Mazor, M. H.; McCammon, J. A.; Lybrand, T. P. *J. Am. Chem. Soc.* **1990**, *112*, 4411–4419.
(72) Auffinger, P.; Wipff, G. *J. Inclusion Phenom. Mol. Recogn.* **1991**, *11*, 71–78.
(73) Auffinger, P.; Wipff, G. *J. Chim. Phys.* **1991**, *88*, 2525–2534.
(74) Marrone, T. J.; Merz, K. M., Jr. *J. Am. Chem. Soc.* **1992**, *114*, 7542–7549.
(75) Olsher, U.; Izatt, R. M.; Bradshaw, J. S.; Dalley, N. K. *Chem. Rev.* **1991**, *91*, 137–164.
(76) Davidson, W. R.; Kebarle, P. *J. Am. Chem. Soc.* **1976**, *98*, 6125–6138.
(77) Ricard, J.; Cornish-Bowden, A. *Eur. J. Biochem.* **1987**, *166*, 255–272.
(78) Arnaud-Neu, F.; Böhmer, V.; Guerra, L.; McKervey, M. A.; Paulus, E. F.; Rodriguez, A.; Schwing-Weill, M. J.; Tabatabai, M.; Vogt, W. *J. Phys. Org. Chem.* **1992**, *5*, 471–481.
(79) Cobben, P. L. H. M.; Egberink, R. J. M.; Bomer, J. G.; Bergveld, P.; Verboom, W.; Reinhoudt, D. N. *J. Am. Chem. Soc.* **1992**, *114*, 10573–10582.
(80) Ting, Y.; Verboom, W.; Groenen, L. C.; van Loon, J.-D.; Reinhoudt, D. N. *J. Chem. Soc., Chem. Commun.* **1990**, 1432–1433.
(81) Lehn, J.-M. *Angew. Chem., Int. Ed. Engl.* **1990**, *29*, 1304–1319.

sated for by the interactions with the encapsulated ion. The calixarene L has some analogy in this respect with lariat ethers,[86,87] synthetic siderophores,[88-91] and their cyclodextrin analogs,[92] polypodands,[93,94] etc.

Considering the negative ΔG and ΔH energies of transfer of the ethyl tetraacetate analog of L and of its Na^+ complex from methanol to acetonitrile, de Namor *et al.*[11] suggested that the possible binding of one MeCN molecule inside the cone could preorganize the calixarene for cation complexation. Whether this "synergistic effect" concerns directly the orientation of the polar binding sites or their coupling via the cone's shape is not clear. Preorganization might concern a solvent-induced higher population of cone/noncone shapes of L, due to complexation of one MeCN molecule. It seems, however, that no such exchange takes place in solution[3,10] and that this effect can be ruled out. One alternative effect of solvent concerns the energy price for (de)solvation of the amide binding sites, which should decrease in the order H_2O > MeOH > MeCN. As a result, L and its carbonyl analogs could be more easily organized in MeCN than in water. This solvent effect is fully supported by MD simulations of the "open" complexes in acetonitrile, compared to water.[36] We have seen that in water, starting from the L(D) complexes only one carbonyl moves to the cation. In acetonitrile solution, three carbonyls rapidly wrap around the cation to form a pseudocavity in which the cation is encapsulated. The energy cost for organizing the pseudocavity is thus lower in acetonitrile than in water.[36]

Preorganization might be also related to more subtle conformational effects, as in spherand complexes,[95] related to the precise conformation of the host. In calixarene complexes, the arrangement of the phenolic oxygens is not the same as in the free ligand: they form a square in the Na^+, K^+, and Cs^+ complexes but an elongated rectangle in uncomplexed L. Interestingly, we find that a MeOH or a MeCN molecule inside the cone is able to induce such an organization. Moreover, the positive free energies of transfer for the free calixarene L[11] from acetonitrile to methanol correlate nicely with its larger affinity calculated *in vacuo* for one MeCN molecule when compared to MeOH. Our calculations on *in vacuo* $SLNa^+$ complexes with a guest inside the cone also give a higher interaction with MeCN than with MeOH (Table III). However, the calculations do not support the thermodynamic consequence of this preorganization effect, if any. We do not find a larger Na^+ affinity for the LMeCN complex compared to the LMeOH complex (Table III). Furthermore, within the $SLNa^+$ complexes, the Na^+–guest interaction is *repulsive* (2.3 kcal/mol for MeOH, 11.7 kcal/mol for MeCN) since the orientation of the cone's guest seems to be determined by the cone rather than by the cation at the lower rim. Notice also that Li^+ needs less symmetrical surroundings than the others M^+ cations. Since a MeCN molecule in the cone induces a squared ether fragment, a *destabilization* of the complex should be observed. This is in disagreement with experimental binding selectivity of ester and ketone analogs of L for Li^+ in acetonitrile.[96] More generally, even if "filling the cone" of calixarenes brings a significant contribution to the solvation and complexation energies, it is clear that solvation cannot be pictured by any single solvent molecule and has enthalpic and entropic components. The fact that the free and Na^+-complexed calixarenes have similar free energies of transfer from methanol to acetonitrile may simply be due to dominant contributions of the cone moiety rather than from similar conformations at the lower rim.

4. The Contribution of the Carbonyl Substituents for Binding the Cations. Carbonyl groups at the lower rim play an important role in cation complexation. Although unsubstituted calixarenes can transport alkali cations through a liquid chloroform membrane,[97,98] they are not efficient cation binders. The Na^+ complex of *p-tert*-butylcalix[4]arene tetramethylether has been characterized by X-ray,[26] but not stability constants are available to our knowledge for this complex. This contrasts with the high binding cation affinities of calixarenes with carbonyl-containing substituents at the lower rim.[13] It is therefore interesting to analyze the cation–calixarene interaction energies $E_{M^+...L}$ within the LM^+ complexes and determine the contribution of the amide groups.

As shown in Tables II and IV–VIII, this contribution is dominant for the hard cations (Li^+, Eu^{3+}) only. It amounts to about 60% (conformer **1**) and 75% (conformer **2**) for LLi^+ and LEu^{3+} complexes in water. For the other complexes ($M^+ = Na^+$, K^+, Cs^+), it is less than the phenolic contribution (35–45%), even in the fully converging (4/0) forms simulated *in vacuo*. In the open-type forms, the amide contribution still decreases as expected (up to 30%). This results from subtle structural features rather than from force field artifacts. The carbonyl contribution is not underestimated, since the charges used on amide oxygens (–0.61) are more negative than those on the ether oxygens (–0.33). In fact, the O=C dipoles can achieve optimal linear arrangements with only small cations and adopt more "tangential coordination" with larger cations.

The cation–ligand attractions depend not only on the nature of the binding sites at the lower rim (*e.g.*, acid/ketone/amide/phosphonamide) but also on the interplay between their precise orientation and the size and charge of the guest. In contrast to tertiary amides like L, secondary amide ligands display low levels of cation extraction,[99] presumably because of internal hydrogen bonding, which competes with a suitable orientation of the binding sites.

5. Anion Coordination to LM^{n+} Complexes. Can the Anion be Neglected? For calixarene complexes, there are few references concerning possible cation–anion interactions. The possible role of the anion on complexation (Cl^- in methanol, ClO_4^- or NO_3^- in acetonitrile[10]), extraction[3,10,12-17] ($X^- = Pic^-$), or transport (with SCN^-) through a CH_2Cl_2 membrane[10] has not been investigated to our knowledge. By using absorption spectroscopy, it was shown that carbonyl-containing calix[4]arenes separate the Na^+Pic^- ion pairs in THF.[3,49] Generally, complexation of the cation by cage compounds is used to separate ion pairs.[101] Examples of anion effects on cation complexation concern mostly crown ethers, which

(82) Lehn, J.-M. In *Perspectives in Coordination Chemistry*; Williams, A. F., Floriani, C., Merbach, A. E., Eds.; Verlag Helvetica Chimica Acta: Weinhem, 1992; pp 447–462.
(83) Cabbines, D. K.; Margerum, D. W. *J. Am. Chem. Soc.* **1969**, *91*, 6540–6541.
(84) McDougall, G. J.; Hancock, R. D.; Boyens, J. C. A. *J. Chem. Soc., Dalton Trans.* **1978**, 1438–1444.
(85) Kodama, M.; Kimura, E. *J. Chem. Soc., Dalton Trans.* **1976**, 116–120.
(86) Gokel, G. W.; Trafton, J. E. In *Cation Binding by Macrocycles*; Inoue, Y., Gokel, G. W., Eds.; Marcel Dekker, Inc.: New York, 1990; pp 253–310.
(87) Gokel, G. W. *Chem. Soc. Rev.* **1992**, 39–47.
(88) Libman, J.; Tor, Y.; Dayan, I.; Shanzer, A.; Lifson, S. *Isr. J. Chem.* **1992**, *32*, 31–40.
(89) Shanzer, A.; Libman, J.; Lifson, S.; Felder, C. E. *J. Am. Chem. Soc.* **1986**, *108*, 7609–7619.
(90) Tor, Y.; Libman, J.; Shanzer, A.; Lifson, S. *J. Am. Chem. Soc.* **1987**, *109*, 6517–6518.
(91) Tor, Y.; Libman, J.; Shanzer, A. *J. Am. Chem. Soc.* **1987**, *109*, 6518–6519.
(92) Coleman, A. W.; Ling, C.-C.; Miocque, M. *Angew. Chem., Int. Ed. Engl.* **1992**, *31*, 1381–1383.
(93) Kron, T. E.; Tsvetkov, E. N. *Russ. Chem. Rev.* **1990**, *59*, 283.
(94) Varnek, A. A.; Maya, A.; Landini, D.; Gamba, A.; Morosi, G.; Podda, G. *J. Phys. Org. Chem.*, in press.
(95) Maye, P. V.; Venanzi, C. *J. Comput. Chem.* **1991**, *12*, 994.
(96) Schwing, M.-J.; McKervey, M. A. In *Calixarenes: a versatile class of macrocyclic compounds*; Vicens, J., Bohmer, V., Eds.; Kluwer Academic Press: Dordrecht, The Netherlands, 1991; pp 149–172.
(97) Izatt, R. M.; Lamb, J. D.; Hawkins, R. T.; Brown, P. R.; Izatt, S. R.; Christensen, J. J. *J. Am. Chem. Soc.* **1983**, *105*, 1782–1785.
(98) Izatt, S. R.; Hawkins, R. T.; Christensen, J. J.; Izatt, R. M. *J. Am. Chem. Soc.* **1985**, *107*, 63–66.
(99) Chang, S. K.; Kwon, S. K.; Cho, I. *Chem. Lett.* **1987**, 987–948.
(100) Ovchinnikov, Y. A.; Ivanov, V. T.; Shkrob, A. M. *Membrane Active Complexones*; Elsevier: Amsterdam, 1974; p 363.
(101) Lehn, J. M. *Acc. Chem. Res.* **1985**, *11*, 49–57.

provide less shielding,[102-107] or Na^+ cryptates in etheral and aromatic solvents.[108]

The poor accessibility of alkali cations to water found in our simulations suggests also that anions like Pic^-, ClO_4^-, and NO_3^- cannot coordinate the complexed M^+ cation. Possible exceptions concern the Li^+ and Eu^{3+} *exo* complexes of calixarenes, which might pair with small anions in nonpolar solvents and could replace binding sites at the lower rim. Alternatively, as suggested by our calculations with SCN^-, some linear or aromatic anions might sit in the upper-rim annuli. This gas-phase picture of the LM^+SCN^- complex may, however, not be relevant in solution. Indeed, in the solid state of the LK^+ complex, SCN^- is outside the cone,[3] which suggests that environmental and solvation effects compete significantly with the SCN^-/LM^+ attraction. The NMR shifts observed upon complexation of NaSCN[3,49] can result from the field of the ions as well as from conformational effects and do not allow us to conclude on the possible inclusion of SCN^- inside the cone. Complexation of harder anions such as F^- inside the cone is still more unlikely, because of the desolvation energy cost.

More critical is the case of the LEu^{3+} complexes in water, where we find four water molecules surrounding Eu^{3+}. Luminescence data are consistent with the coordination of one water molecule only to Eu^{3+}.[18,19,109,110] The difference between experimental and calculated values may be due to $Eu^{3+}\cdots Cl^-$ coordination in water and to the neglect of anions in our simulation. Indeed, solvent molecules and anions like F^- or phosphate influence the lifetime of luminescence by entering the first coordination sphere of M^{3+} cations complexed by cryptands.[110,111] Such ion pairing is also consistent with MD simulations on the complex of cryptand 222 with $EuCl_3$ in water, which show that at least two anions form intimate ion pairs with the Eu^{3+} cation.[112] The neglect of anions in water is therefore justified for alkali cation complexes but not for lanthanide complexes.

The calixarenetetraamide L complexes substantially alkaline earth cations in methanol,[5] with Cl^- or ClO_4^- as anions. As in the trivalent series, but to a lesser extent, these anions might also be involved in the structure of the complexes.

6. Inclusion of Neutral Molecules in the Cone of Calixarenes. Our gas-phase results and solid-state structures[7,8,22,24,113-115] show that calix[4]arenes can bind a neutral guest (*e.g.*, solvent molecules) inside the cone. In solution, there is no direct proof of such complexation. The NMR downfield shift of aromatic protons of calix[4]arenetetraacetate observed in acetonitrile (but not in CD_3OD or $CDCl_3$) is consistent with the "shaping effect" of one MeCN inside the cone and the high MeCN/L interaction energy, compared to the MeOH/L interaction. As found here in water and in acetonitrile,[36] it is likely that solvent molecules of appropriate size and shape should fill the cone.

The energy-minimized complexes with a neutral guest are such that the O–H bond of water or the CH_3 groups of methanol and acetonitrile are more or less perpendicular to one phenolic ring of L, *i.e.*, as if there were hydrogen-bonding to a π system. Such C–H/π interactions have been shown to be an important driving force for host–guest complexation in apolar organic media.[116] Some molecular mechanics simulations used a Morse-like potential for CH_3/π interaction to model the inclusion pyridine complex of a calix–crown.[30]

Our results obtained with a simple 1–6–12 potential suggest no need for a special term for CH_3/π interactions if the force field is appropriate and if all geometry parameters are relaxed properly. The driving forces of complexation are both van der Waals and electrostatics. Dipole–dipole interactions orient the dipole moment of the guest in the cone opposite that of phenolic fragments, and dipole–quadrupole interactions may account for C–H/π orientation. In the case of aromatic guests, such electrostatics account for "offset π-stacked" and "edge-on" stabilizing interactions between the guest and phenolic fragments of calixarene.[117]

Conclusions

Structural information is essential for understanding the recognition properties of synthetic receptors and for designing new classes of ionophores. Our best knowledge rests on X-ray structures in the solid state. In solution, the precise conformations are not known from experiment. In particular, it is not clear whether symmetrical forms observed on the NMR time scale are time averages of asymmetric ones or correspond to real energy minima. Our computer investigation on the complexes of calixarenetetraamide in the gas phase and in aqueous solution reveals their flexibility and mobility.

Although all structures seem quite rigid and retain their cone shape, two kinds of motions have been characterized. First, the cone itself can evolve from C_4 forms to C_2 forms which are more or less elongated, depending on the presence of a molecular guest and on the cation complexed at the lower rim. Mechanical coupling between the top and bottom is observed as a dynamic process, as well as in instant or average structures. Second, the most important feature concerns the flexibility of amide moieties at the lower rim. The solid-state picture of the calixarene consists of diverging carbonyls in the free state and fully converging carbonyls in the K^+ complex. The simulations demonstrate the versatility of the cationic binding sites, which are not preorganized for complexation. In solution, the fully convergent form of cation complexes may not be the most stable one and is at least in equilibrium with other partially open complexes. As in crown ether or cryptate complexes,[118] conformations differ from one cation to the next. For calixarenes, they can also be solvent-dependent, via the modulation of the cone shape after inclusion of solvent molecules and the solvation of the partners.

It is stressed that flexibility of the ligand is important to provide optimal surrounding of the complexed cation, as well as to facilitate ionophoric processes. It lowers kinetic barriers for complexation/decomplexation by providing relays for (de)solvation of the ion and of the ligand. Our simulations suggest that calixarenes with flexible pseudo-cavities like L or analogs (*e.g.*, esters, thioamides, thioesters, phosphoryl oxygens[79]) may be particularly efficient.

From the computational side, these simulations demonstrate the need for explicit representation of the solvent to model complexation and recognition processes. Flexibility of the pseudo-cavity can make free energy calculations on small time scales

(102) Wong, K. H.; Konnitzer, G.; Smid, J. *J. Am. Chem. Soc.* **1970**, *92*, 666–670.
(103) Takaki, U.; Smid, J. *J. Am. Chem. Soc.* **1971**, *93*, 6760–6765.
(104) Chen, G.; Wallage, W.; Eyring, E. M.; Petrussi, E. M. *J. Phys. Chem.* **1984**, *88*, 5545–5550.
(105) Tsivadze, A. Y.; Varnek, A. A.; Khutorsky, V. E. *Coordination Compounds of Metals with Crown-Ligands*; Nauka Publishing House: Moscow, 1991; p 397.
(106) Zavada, J.; Rechanec, V.; Stibor, I.; Viteck, A. *Collect. Czech. Chem. Commun.* **1985**, *50*, 1184–1186.
(107) Zavaeva, J.; Rechanec, V.; Kosian, D. *Collect. Czech. Chem. Commun.* **1983**, *48*, 2509–2513.
(108) Nakamura, K. *J. Am. Chem. Soc.* **1980**, *102*, 7846–7848.
(109) Pottle, C.; Pottle, M. S.; Tuttle, R. W.; Kinch, R. J.; Scheraga, H. A. *J. Comput. Chem.* **1980**, *1*, 46–58.
(110) Sabatini, N.; Guardigli, M.; Lehn, J.-M.; Mathis, G. *J. Alloys Compds.* **1992**, *180*, 363–367.
(111) Sabatini, N.; Peratoner, S.; Latanzi, C.; Delonte, S.; Balzani, V. *J. Phys. Chem.* **1987**, *91*, 6136–6139.
(112) Troxler, L.; Wipff, G., unpublished results. See also ref 121.
(113) Andreetti, G. D.; Ugozzoli, F. In *Calixarenes: a versatile class of macrocyclic compounds*; Vicens, J., Bohmer, V., Eds.; Kluwer Academic Publishers: Dordrecht, The Netherlands, 1991; pp 87–123.
(114) Andreetti, G. D.; Ugozzoli, F. *Gazz. Chim. Ital.* **1989**, *119*, 47–50.
(115) Andreetti, G. D.; Pochini, A.; Ungaro, R. *J. Chem. Soc., Perkin Trans. II* **1983**, 1773–1779.
(116) Kobayashi, K.; Asakawa, Y.; Kato, Y.; Aoyama, Y. *J. Am. Chem. Soc.* **1992**, *114*, 10307–10313.
(117) Hunter, C. A.; Sanders, J. K. M. *J. Am. Chem. Soc.* **1990**, *112*, 5525–5534.
(118) Dobler, M. *Ionophores and their Structures*; Wiley Interscience: New York, 1981.

problematic because of sampling difficulties. With present computer performances, however, this challenging problem should be solved.[119]

Acknowledgment. The authors are grateful to CNRS and to the CNRS-IBM scientific group for computer time at the CIRCE. A.V. thanks the MRT and the Rhone-Poulenc company for a BRITEST grant, and P.G. thanks the CEA for a grant. We thank E. Engler for kind assistance in computer graphics and Dr. K. Russell for linguistic assistance.

(119) McCammon, J. A. *Science* **1987**, *238*, 486–491; *Annu. Rev. Phys. Chem.* **1992**, *43*, 407–435.
(120) Burgess, J. *Metal Ion in Solution*; Ellis Horwood: Chichester, U.K., 1978.
(121) Wipff, G. *J. Coord. Chem.* **1992**, *27*, 7–37.